AD-A169 698 CERAMIC BARRIER TURBINE BLADE DEMONSTRATION(U) ROCKWELL 1/1
INTERNATIONAL CANOGA PARK CA ROCKETDYNE DIV D SHEA
MAY 86 RI/RD86-150 MTL-TR-86-17 DAAG46-84-C-0002

UNCLASSIFIED F/G 11/2 NL

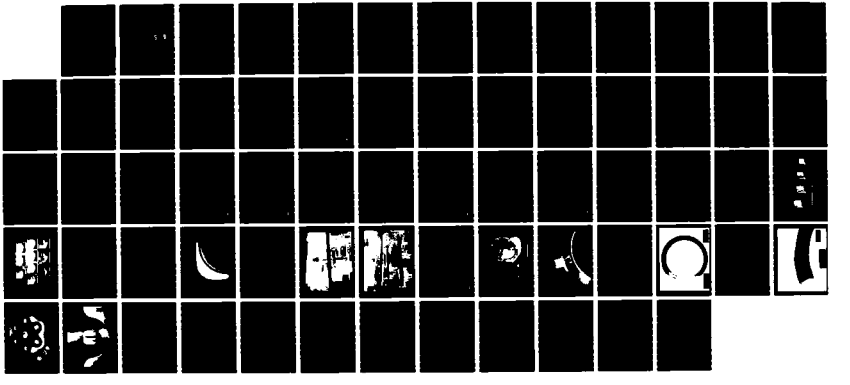

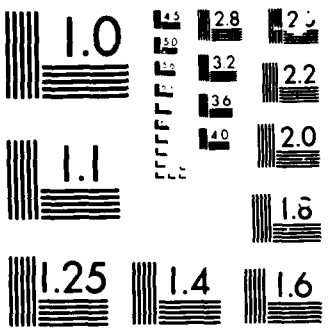
1.0
1.1
1.25
1.4
1.6
2.8
3.2
3.6
4.0
2.2
2.0
1.8

(2)

US ARMY
LABORATORY COMMAND
MATERIALS TECHNOLOGY
LABORATORY

AD

MTL TR 86-17

CERAMIC BARRIER TURBINE BLADE DEMONSTRATION

May 1986

DANIEL SHEA
Rockwell International
Rocketdyne Division
Canoga Park, California 91303

FINAL REPORT

Contract DAAG46-84-C-0002

Prepared for

U.S. ARMY MATERIALS TECHNOLOGY LABORATORY
Watertown, Massachusetts 02172-0001

The findings in this report are not to be construed as an official Department of the Army position, unless so designated by other authorized documents.

Mention of any trade names or manufacturers in this report shall not be construed as advertising nor as an official indorsement or approval of such products or companies by the United States Government.

DISPOSITION INSTRUCTIONS

Destroy this report when it is no longer needed
Do not return it to the originator.

UNCLASSIFIED

SECURITY CLASSIFICATION OF THIS PAGE (When Data Entered)

REPORT DOCUMENTATION PAGE

READ INSTRUCTIONS BEFORE COMPLETING FORM

1. REPORT NUMBER: MTL TR 86-17	2. GOVT ACCESSION NO.
3. RECIPIENT'S CATALOG NUMBER	
4. TITLE (and Subtitle): CERAMIC BARRIER TURBINE BLADE DEMONSTRATION	5. TYPE OF REPORT & PERIOD COVERED: Final Report 1/84 to 3/86
6. PERFORMING ORG. REPORT NUMBER: RI/RD86-150	
7. AUTHOR(s): Daniel Shea	8. CONTRACT OR GRANT NUMBER(s): DAAG46-84-C-0002
9. PERFORMING ORGANIZATION NAME AND ADDRESS: Rockwell International, Rocketdyne Division, Canoga Park, California 91303	10. PROGRAM ELEMENT, PROJECT, TASK AREA & WORK UNIT NUMBERS: D/A Project: 1L162105AH84
11. CONTROLLING OFFICE NAME AND ADDRESS: U.S. Army Materials Technology Laboratory, ATTN: SLCMT-ISC, Watertown, Massachusetts 02172-0001	12. REPORT DATE: May 1986
	13. NUMBER OF PAGES: 53
14. MONITORING AGENCY NAME & ADDRESS (if different from Controlling Office)	15. SECURITY CLASS. (of this report): Unclassified
	15a. DECLASSIFICATION/DOWNGRADING SCHEDULE

16. DISTRIBUTION STATEMENT (of this Report)

Approved for public release; distribution unlimited.

17. DISTRIBUTION STATEMENT (of the abstract entered in Block 20, if different from Report)

18. SUPPLEMENTARY NOTES

19. KEY WORDS (Continue on reverse side if necessary and identify by block number)

Ceramics
Gas turbines
Silicon nitride
Mechanical properties
Processing

20. ABSTRACT (Continue on reverse side if necessary and identify by block number)

SEE REVERSE

DD FORM 1 JAN 73 1473 EDITION OF 1 NOV 65 IS OBSOLETE

UNCLASSIFIED

SECURITY CLASSIFICATION OF THIS PAGE (When Data Entered)

Block No. 20

ABSTRACT

The next generation of gas turbine engines will operate at temperatures that exclude using uncooled metal alloys for the turbine blades. Cooling of theses blades is not the optimum approach because the large coolant flow requirements will adversely affect engine efficiency. The Ceramic Barrier Turbine Blade program has successfully shown that a thermal barrier can be incorporated into the blade to shield the metal components from the hot turbine gases and greatly reduce coolant flow requirements. The principal component of this thermal barrier is a thin silicon nitride shell which envelopes a cooled metal core. Combining ceramic and metal materials into a single design was achieved by mounting the ceramic shell loosely over the structural metal core and retaining it with a cap at the blade tip. Loads on the shell are compressive, allowing the use of light, thin-walled sections. A novel two-layer insulating/cooling system is used to maintain the internal temperature 1000 F below the turbine operating temperature. The design features of the ceramic barrier turbine blade and the fabrication processes are described. Results of the successful spin test conducted to demonstrate concept feasibility are presented.

PREFACE

This is the final technical report of the Ceramic Barrier Turbine Blade Demonstration Program initiated and funded through the Army Research and Technology Office, Dr. Charles Church, Assistant Director. The program was conducted under Contract Number DAAG46-84-C-0002 for the Army Material Technology Laboratory and was monitored by Dr. R. Nathan Katz, Chief, Ceramics Research Division.

TABLE OF CONTENTS

LIST OF FIGURES

LIST OF TABLES

PREFACE

This is the final technical report of the Ceramic Barrier Turbine Blade Demonstration Program initiated and funded through the Army Research and Technology Office, Dr. Charles Church, Assistant Director. The program was conducted under Contract Number DAAG46-84-C-0002 for the Army Material Technology Laboratory and was monitored by Dr. R. Nathan Katz, Chief, Ceramics Research Division.

TABLE OF CONTENTS

LIST OF FIGURES

LIST OF TABLES

SUMMARY

The Ceramic Barrier Turbine Blade program demonstrated that a composite ceramic and metal turbine blade is a viable candidate for the next generation of high temperature turbines. The program was structured to design: a ceramic barrier turbine blade that met the requirements of an existing turbine engine operating at an inlet temperature of 2650 F; produce samples of the thin walled ceramic shells; and ambient spin test these shells at turbine operating speeds.

The ceramic barrier turbine blade assembly consists principally of a silicon nitride outer shell, a stagnant insulating air layer, a metallic coolant liner, an active coolant layer, and a metallic inner core. This thermal barrier system allows the turbine blade to operate at 2650 F and is capable of operating at over 2900 F, without exceeding the engine coolant flowrate limits.

Because the Ceramic Barrier Turbine Blade uses both a metal footing and end cap, it can directly replace a cooled metal blade without significant modification of the engine. For this reason, the Ceramic Barrier Turbine Blade can be developed at relatively lower cost compared to monolithic ceramic blades and allows the use of existing testbed engines and facilities.

The Ceramic Barrier Turbine Blade combines the temperature tolerance of ceramics with the high strength of metal alloys at moderate temperatures. This blade design utilizes a thin wall (0.015 inch) silicon nitride shell to shield the internal metal components from the hot turbine gases. The shell is loosely mounted but held in position at the tip by a metal end cap. The loading of the shell is in compression, taking advantage of the 400 ksi compressive strength of silicon nitride. The "loose" mounting of the shell eliminates problems due to differential expansion of the metal and ceramic components. The shell is protected from tip rubbing stresses allowing the use of small tip clearances to minimize flow losses while increasing turbine blade reliability and life.

Samples of the silicon nitride shell were produced using low cost, net shape injection molding and sintering processes. They were proof spin tested to an overspeed condition of 60,000 rpm at a 5.8 inch diameter to verify their integrity. At this speed, the effective weight of the shell increased from 0.002 lbs at rest to over 800 lbs due to the centrifugal force. All of the ceramic shells passed this proof test. The factor of safety for the shells under these conditions was 19 with a probability of survival of 99.5%. These results were obtained using a compressive strength of 150 ksi.

INTRODUCTION

To achieve major increases in power and fuel efficiency, the operating temperature of the next generation gas turbine engine will be increased by 450 F. Advances in materials and design technology are required to develop components that can operate at turbine inlet temperatures of 2600 F. Projected improvements in metals technology can support only modest increases in operating temperature for components such as the turbine blade. Active cooling flowrate requirements for these blades would be so high that they cancel any potential for increased engine efficiency. The Ceramic Barrier Turbine Blade concept can safely operate at these conditions and increase overall engine efficiency.

The Ceramic Barrier Turbine Blade design combines ceramic and metal components into a single blade for high heat tolerance and high tensile strength. This concept use a unique two layer insulating/cooling system that keeps the metal structural core at a safe operating temperature. A silicon nitride outer barrier shields the internal components from the hot turbine gases. The ceramic barrier is retained in compression by a flange at the outer diameter.

Turbine blades must possess high tensile strength to withstand the loading due to the high rotational speed. A combined ceramic/metal turbine blade has two to four times greater tensile strength than a monlithic ceramic blade. The Ceramic Barrier Turbine Blade use a metal footing for attachment to the rotor. The tip of the blade has a metal end cap that protects the ceramic shell from damage due to tip rubbing. Because of these features, the Ceramic Barrier Turbine Blade can be a direct replacement for a cooled metal turbine blade.

The objective of this program was to verify that the Ceramic Barrier Turbine Blade is a viable candidate for use in the next generation of high temperature turbine engine. The program was structured into three technical tasks: design and analysis; hardware fabrication; and test. The design and analysis task effort included designing a Ceramic Barrier Turbine Blade for operation in an existing engine. Analytical effort verified the blade performance and structural integrity. The hardware fabrication task identified key components and demonstrated that they could be produced. The test effort was an ambient proof spin test of the ceramic shells.

DISCUSSION

DESIGN AND ANALYSIS

The results of the design and analysis effort are presented in this section. This includes the selection of the baseline turbine blade and a description of the components and their function. The results of the thermal and structural analyses are presented along with a component producibility study.

BASELINE TURBINE BLADE

The Ceramic Barrier Turbine (CBT) Blade was designed for an existing gas turbine engine in which high temperature capability was being incorporated. The baseline engine is the F107, currently used to power the Air Force cruise missile. This engine is produced by the Williams International Company, Walled Lake, Michigan, and an agreement was entered into for incorporating the CBT blade into this engine. A hot spin test rig is available for testing the upgraded components under simulated turbine conditions. Williams has developed several turbine blades for use in this engine. The one on which the CBT blade was baselined is referred to as the TACOM configuration. This blade configuration was selected because it had active cooling capability.

The operating conditions for the upgraded engine and turbine blade data are shown in Table 1.

TABLE 1. ENGINE CHARACTERISTICS

Turbine inlet temperature	2650 F	Blade height	0.70 inches
Shaft speed	57,000 rpm	Number of blades	40
Horsepower	120 hp	Chord length	0.75 inches
Bleed air temperature	500 F	Tip diameter	5.70 inches

In addition to meeting these operating requirements, the Ceramic Barrier Turbine Blade was designed to utilize the following producibility requirements:

- o Proven ceramic and metal technologies
- o Current, low cost manufacturing processes
- o High volume production adaptability

The Ceramic Barrier Turbine Blade developed during this program is an attempt to use compressively loaded, thin walled ceramic technology in turbine engine rotor design. While producing a turbine blade to fit the envelope of the F107 engine, the complexity of the blade profile was reduced to keep design,

analysis, and fabrication effort within the scope of this program. The profile changes included the elimination of leading edge and trailing edge twist, elimination of the hub to tip taper, and an increase to the midsection blade thickness. The differences between the baseline blade and the Ceramic Barrier Turbine Blade are shown in Figure 1. The final blade profile was reviewed by Williams International and found to be acceptable for use in the F107 engine.

CERAMIC BARRIER TURBINE BLADE CONCEPT

The Ceramic Barrier Turbine Blade is composed of several components assembled into an effective high temperature turbine blade. The turbine blade is built around an inner core (Figures 2a and 2b) made from high strength MAR-M-246. The end of the core has a flange upon which the the ceramic shell seats during spinning. This part of the core is referred to as the end cap. The end cap has three functions: retention of the ceramic shell and transfer of loads into the core; containment of the exhaust ports for the cooling airflow; and protection of the ceramic shell from the effects of blade tip rubbing on the outer shroud.

The ceramic shell, made from silicon nitride, forms the aerodynamic outer profile of the blade. In addition to extracting the work from the turbine gases, the shell forms the outer layer of the thermal barrier. This shell is made from net shape injection molded silicon nitride, between 0.015 and 0.020 inches thick. It is not bonded or joined to the core but is held in position by the centrifugal forces forcing it outwards against the end cap. This eliminates the possibility of stresses developing at the ceramic/metal interface due to differential thermal expansion.

To prevent binding of the ceramic shell on the end cap, a thin washer called the "friction reducing layer" is inserted between these parts. The washer is made from Haynes 25, a cobalt-based material, that has a low coefficient of friction against the silicon nitride shell. It allows small sliding adjustments between the parts during thermal growth.

The thermal resistance barrier is composed of two zones separated by the coolant liner. Cooling air bleed from the engine's compressor is circulated through the inner zone next to the core. A low coolant flowrate carries away the small amount of heat that passes through the highly effective insulating outer zone. The outer zone is referred to as the stagnant air gap. This air gap, approximately 0.015 inches thick, acts as an insulator across which little heat is transferred due to the low heat conducting properties of air. An opening at the base of the ceramic shell allows the pressure of the stagnant air gap to equalize with the turbine gas pressure. The outer shell, which contains the stagnant air gap, must be made from ceramic materials since it is not cooled and must be capable of surviving at temperatures up to 2650 F.

All of the metal components are shielded by the ceramic shell by the turbine gases except for the end cap. This blade component is not directly exposed to the mainstream turbine gases because it operates in a cooled boundary layer

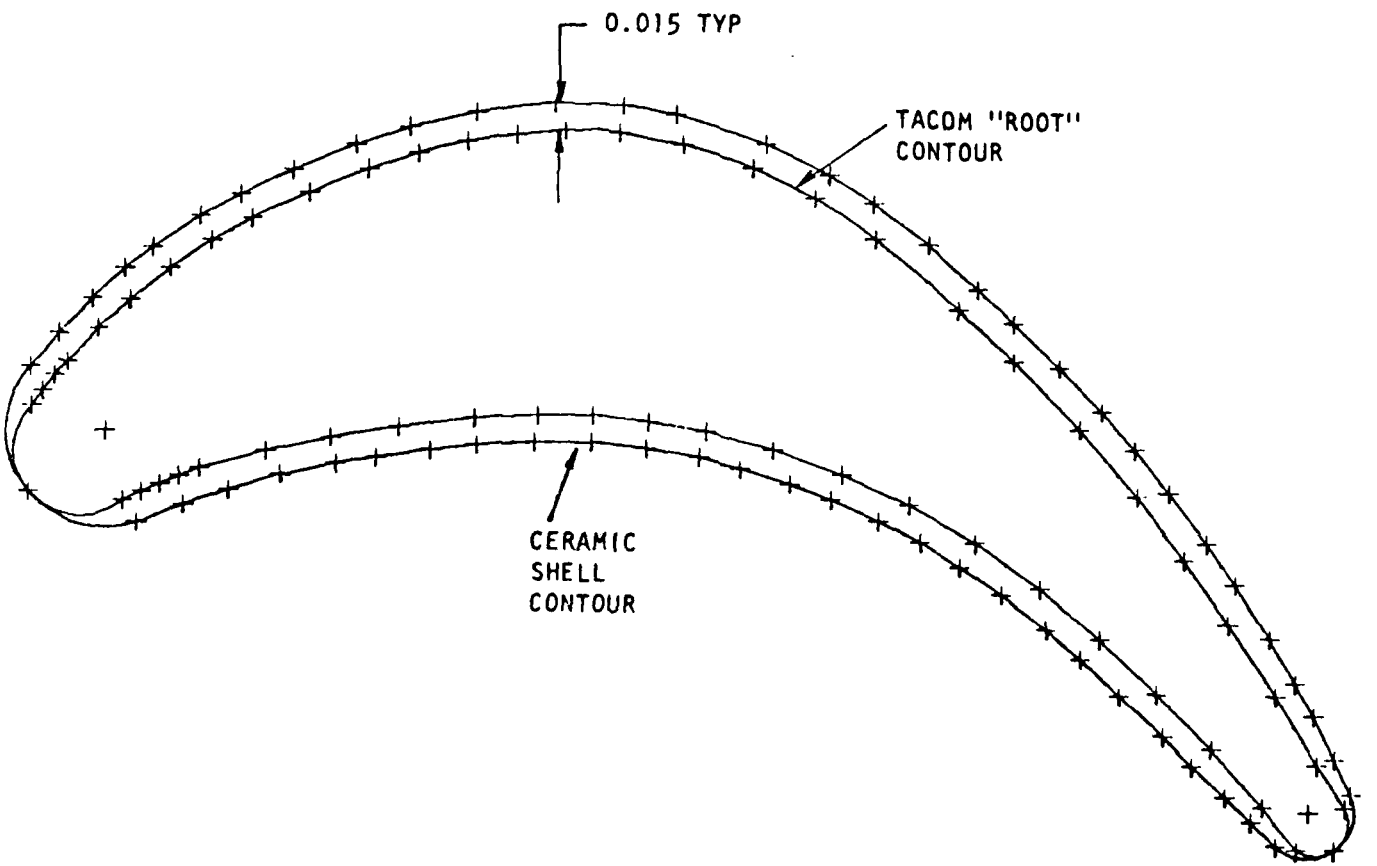

FIGURE 1

BLADE PROFILE COMPARISON

CERAMIC BARRIER TURBINE BLADE CONCEPT

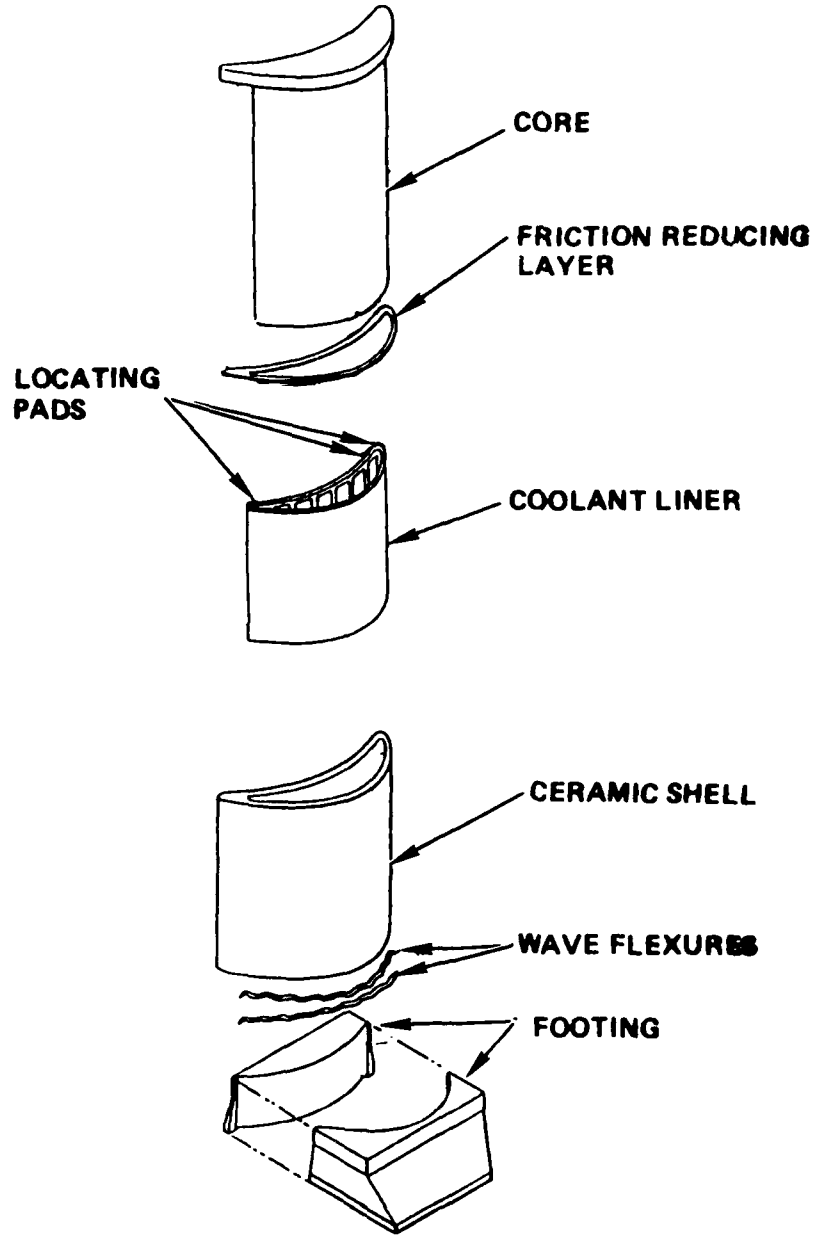

Rockwell International
Rocketdyne Division

FIGURE 2A

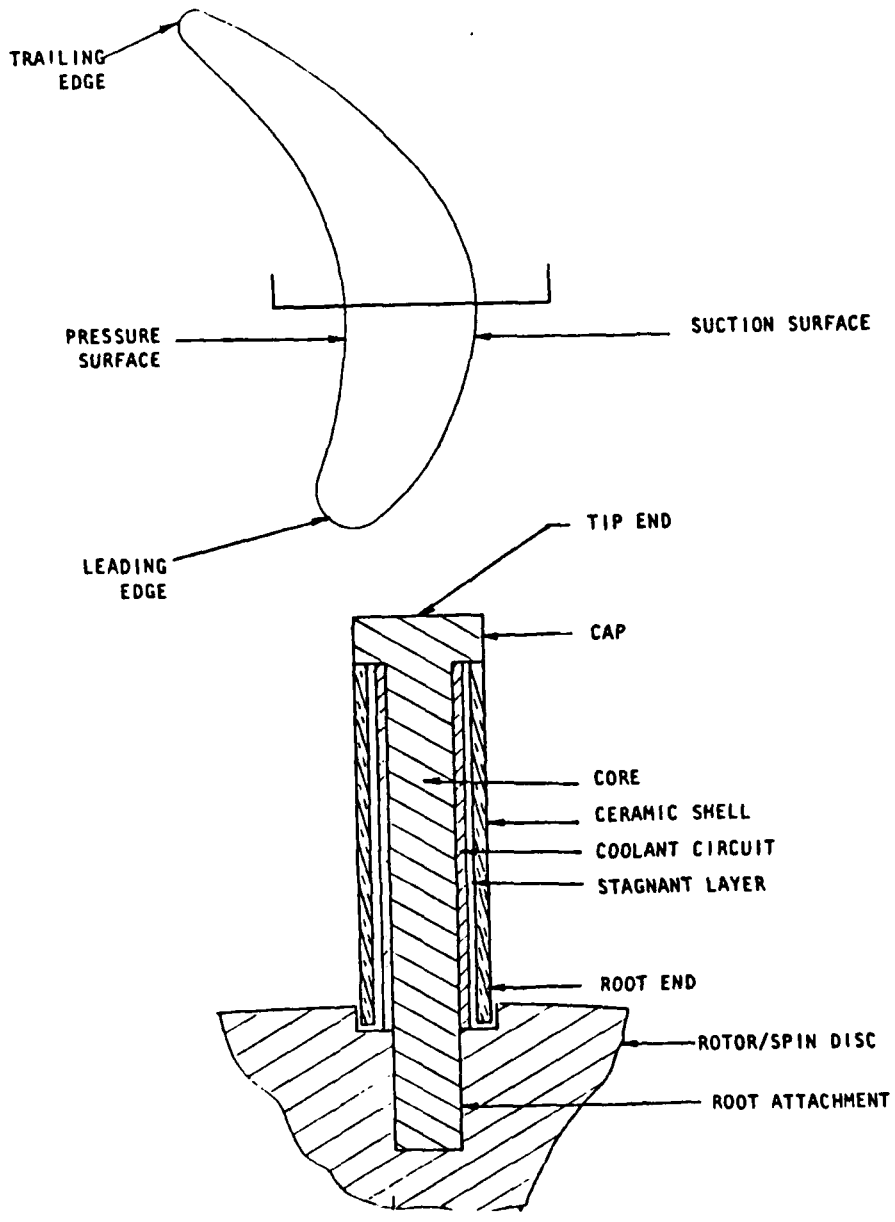

FIGURE 2B

BASIC ASSEMBLED CONFIGURATION

next to the outer wall. This boundary layer is formed from cooling air injected through the combustor and nozzle walls to keep these components cooled. The temperature of the boundary layer when it reaches the turbine blades is 1800 F. Additional cooling of the end cap is provided by the exhaust of the inner zone cooling air through the end cap.

COMPONENT FEATURES

Ceramic Shell

The ceramic barrier, or shell, is made from injection molded and sintered silicon nitride (Si_3N_4). This shell forms the blade's aerodynamic profile (Figure 3). The silicon nitride shell is directly exposed to the hot mainstream turbine gases and remains at a high temperature throughout operation. Silicon nitride was selected for its combination of high strength at these temperatures and its superior thermal shock resistance properties. The silicon nitride shells have high resistance to erosion and its strength properties are not diminished due to long term exposure to high temperature.

A thin walled section is used to minimize the weight of the ceramic shell. A wall thickness of 0.015 inches is the practical minimum for injection molding parts of this size. The strength of the silicon nitride in compression is illustrated by the fact that the shell, weighing 0.002 lbs. at rest, will have an effective weight of 800 lbs-force due to centrifugal loading. The stress on the shell at this loading is still only 5% of the design strength.

The thickness of the ceramic shell is increased from 0.015 inches at the hub to 0.020 inches at the tip. The change in thickness provides a slope on the interior profile to prevent the shell from hanging up on the mold during injection molding. Sloping of the exterior surfaces is not required.

The inner and outer surfaces of the ceramic shell are molded to their net shape. No additional machining or surface treatment is required after injection molding and sintering of the part. Final machining of these parts is limited to grinding the end.

End Cap

The end cap is the flanged portion of the core against which the ceramic shell seats. Although referred to as a separate item, it is actually an integral part of the metallic core, as shown in Figure 4. The seating surface is machined flat and smooth to eliminate discontinuities that can cause potentially damaging stresses in the ceramic shell.

The end cap contains the exhaust holes for the inner zone cooling air. One hole is provided for each cooling passage and the size of each hole is varied to act as an orifice, controlling the coolant flowrate through each passage. The cooling air which exits from these holes helps cool the end cap.

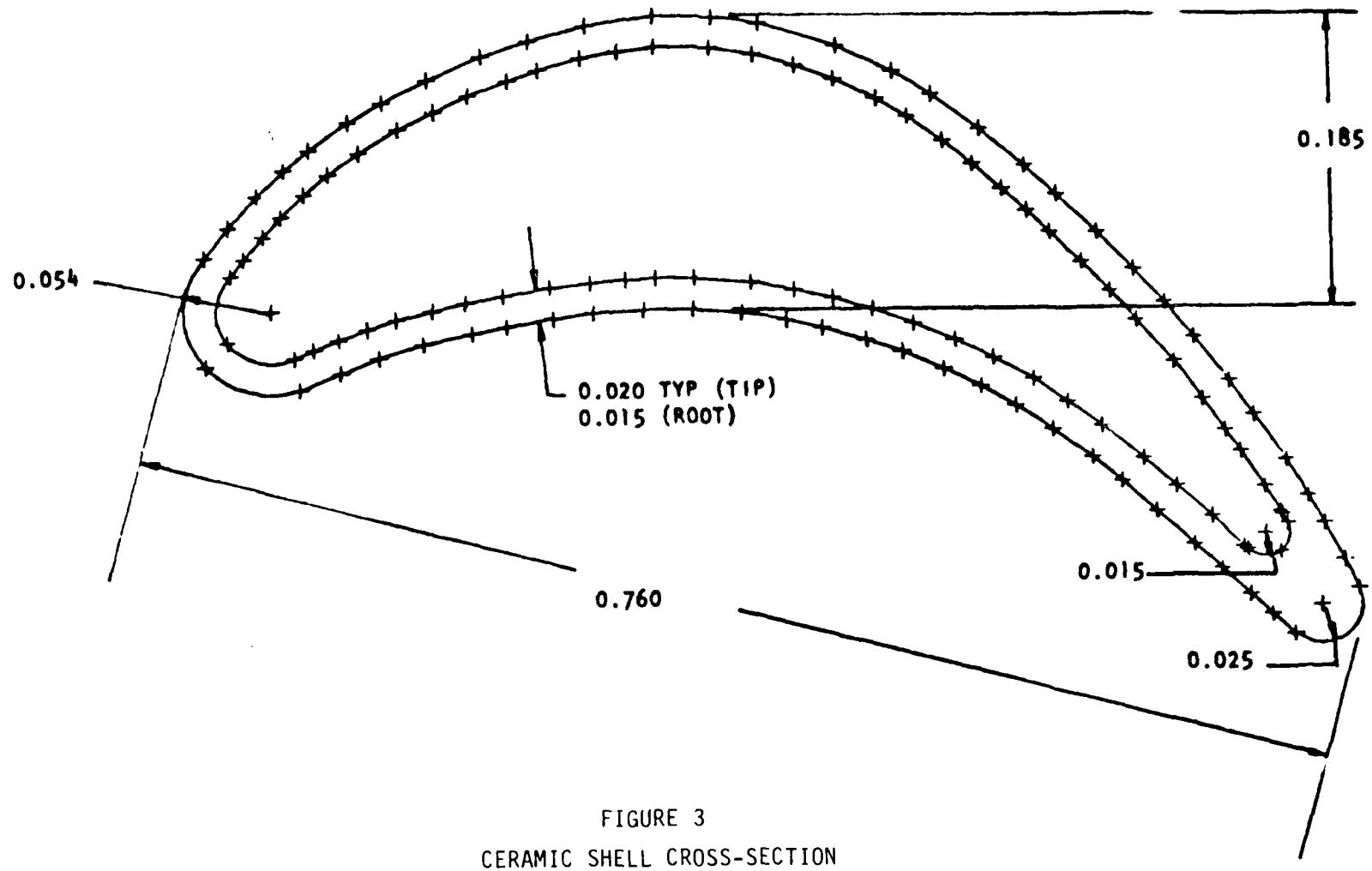

FIGURE 3
CERAMIC SHELL CROSS-SECTION

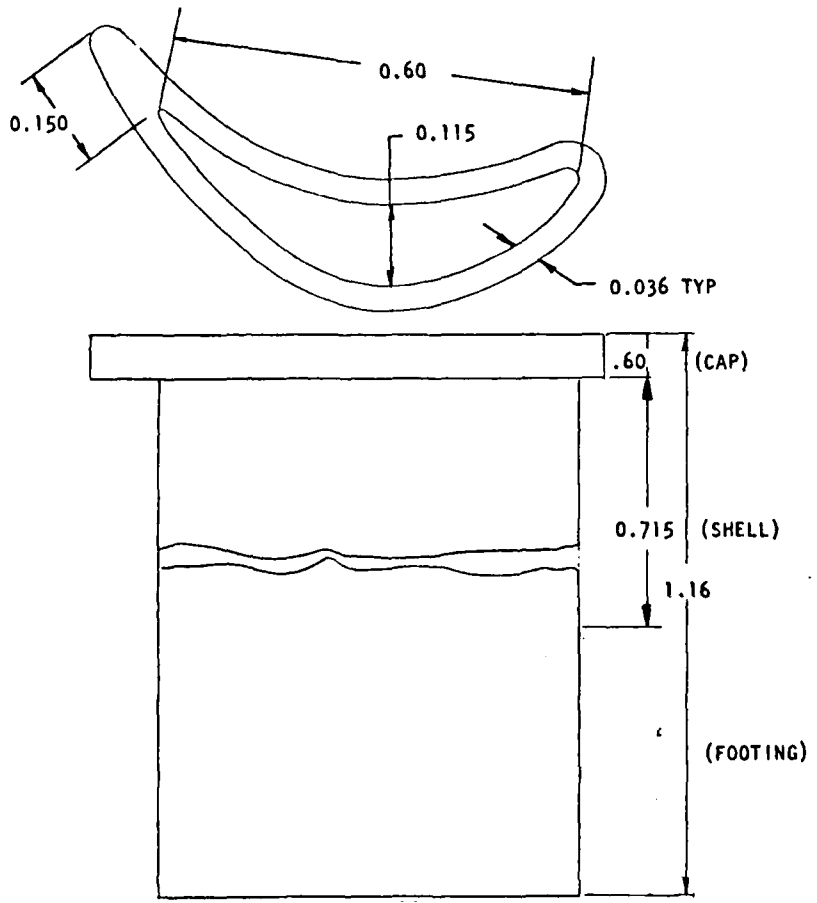

FIGURE 4

INTEGRAL CORE/CAP GEOMETRY

The metal end cap protects the shell from rubbing damage during operation. The F107 turbine uses an unshrouded rotor design and small tip clearances are maintained to minimize flow losses around the tip. The ends of the blade occasionally rub against the tip seal. At engine operating speeds, a ceramic turbine blade that rubs against the tip seal would fail. The metal end cap isolates the shell such that all rubbing loads are carried by the metal end cap and core.

Friction Reducing Layer

A thin washer, referred to as the "Friction Reducing Layer" (FRL), is inserted between the ceramic shell and the end cap. As the turbine blade is heated the MAR-M-246 end cap expands at a greater rate than the silicon nitride shell. If the two parts were locked together, the end cap expansion would cause failure of the ceramic shell. The FRL (approximately 0.010 inches thick) allows these two materials to slide freely.

A thin FRL is used to minimize its deformation due to loading by the ceramic shell. The material from which the washers are made has a low coefficient of static friction against silicon nitride at high temperature. A prior study[1] tested numerous materials and found that cobalt based alloys have the lowest friction coefficient against silicon nitride. Materials such as Stelite 6B and Haynes 25 are suitable for this component.

Metallic Core

The metallic core is the main structural component of the CBT blade, carrying the weight of the ceramic shell, the end cap, and the coolant liner. The configuration of the core is shown in Figure 4. The references along the length of the core show the location of the other components after assembly. The core is made from currently available turbine blade materials such as MAR-M-246, which have high strength at high temperatures. During operation, the core is maintained at 1500 F. This temperature is below the operating limit for this material.

Coolant Liner

The coolant liner is a sheet of alloy 718 that is attached to the surface of the core and separates the active cooling passages from the stagnant air gap. Figure 5 shows a cross-section of the blade and the location of the coolant liner. A series of integral ribs along the length of the liner provide for a 0.006 inch gap through which cooling air is circulated from the base to the tip. The cooling passages are wide, relatively flat channels to provide coverage over as large an area of the core as possible. The size and number of ribs are minimized to reduce direct heat transfer to the core via conduction.

---

1 Ceramic Gas Turbine Engine Demonstration Program, Garrett Turbine Engine Company, Contract No. N00024-76-C-5352

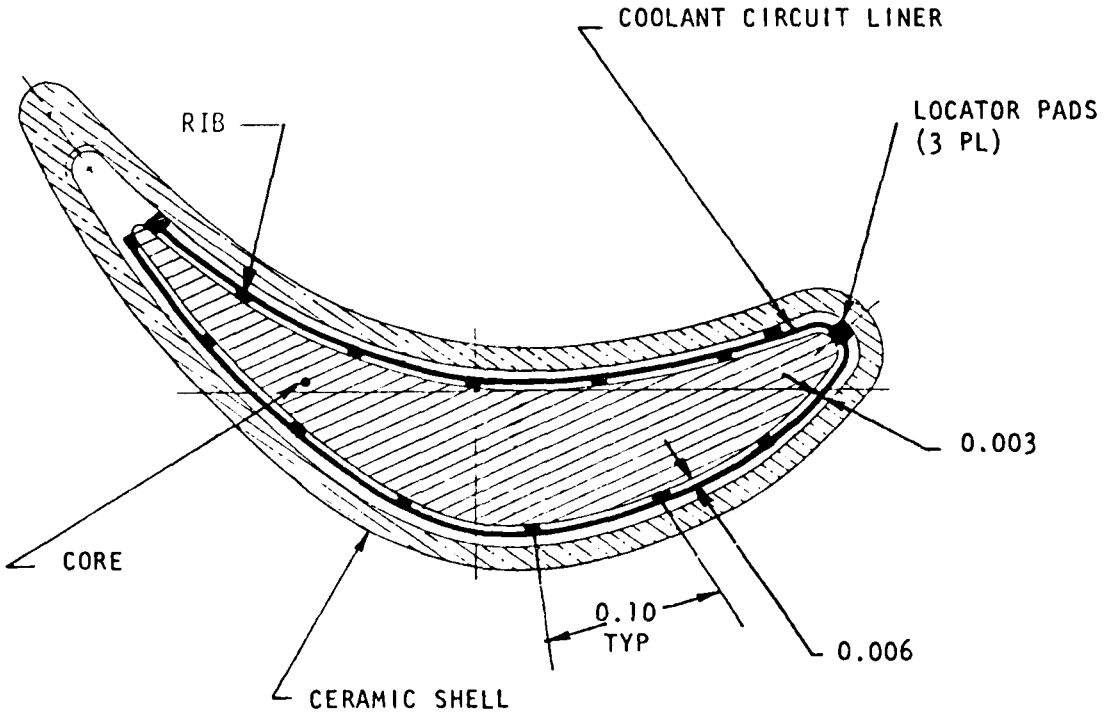

FIGURE 5

COOLANT LINER CROSS-SECTION (INSTALLED)

Wave Flexure

The wave flexure is used to keep the ceramic shell seated against the end cap when the turbine is not spinning. This component fits in the space between the bottom of the shell and the blade footing and can be thought of as a weak wavey spring. The static loading of this component prevents shifting of the shell during the cooling down period after engine operation. The weight of the flexure does not add significantly to shell loading during operation.

Locating Tabs

Three small tabs of alloy 718 are brazed onto the coolant liner at the blade tip. One of them is placed on the leading edge while the other two are placed on the pressure side leading and trailing edges as shown in Figure 5. These tabs keep the ceramic shell from shifting out of position during engine startup. If these tabs were not provided, the turbine gases would cause shifting of the shell location before it had been seated by the centrifugal forces. Only three tabs are required to assure the correct positioning of the shell. The tabs are small to minimize contact with the ceramic shell.

THERMAL ANALYSIS

Thermal analysis was performed to determine the coolant flowrate requirements for the Ceramic Barrier Turbine Blade for maintaining the internal core at a temperature less than 1500 F. Various locations along the blade were studied. All calculations were performed under steady state conditions.

Three areas along the blade length were initially studied in detail. The analysis was then limited to the suction side, after initial calculations found these temperatures were higher than the corresponding locations on the pressure side. The areas studied are shown in Figure 6. Each section that was modeled included one cooling passage and one half of the rib on either side of the passage. The height of each model extended from the base of the ceramic shell to the tip of the shell.

The thermal analysis utilized a two-dimensional planar finite element analysis model. A sample of the finite element model is shown in Figure 7. The end cap, the friction reducing layer, the wave flexure, or the locating tabs operate in the wall boundary layers and do not see the mainstream gases. These components were not included in the analysis.

Heat transfer coefficients between the turbine gases and the skin of the ceramic shell were determined from a NASA report[2]. The coefficient varied around the blade profile, with the leading edge suction side having the higher transfer coefficient. The transfer coefficient reduces to approximately one half at the midpoint of the blade and is further reduced at the trailing edge. This analysis conservatively assumes a constant gas temperature around the blade.

---

2 Design and Analysis of Cooled Turbine Blades, NASA publication CR-72417

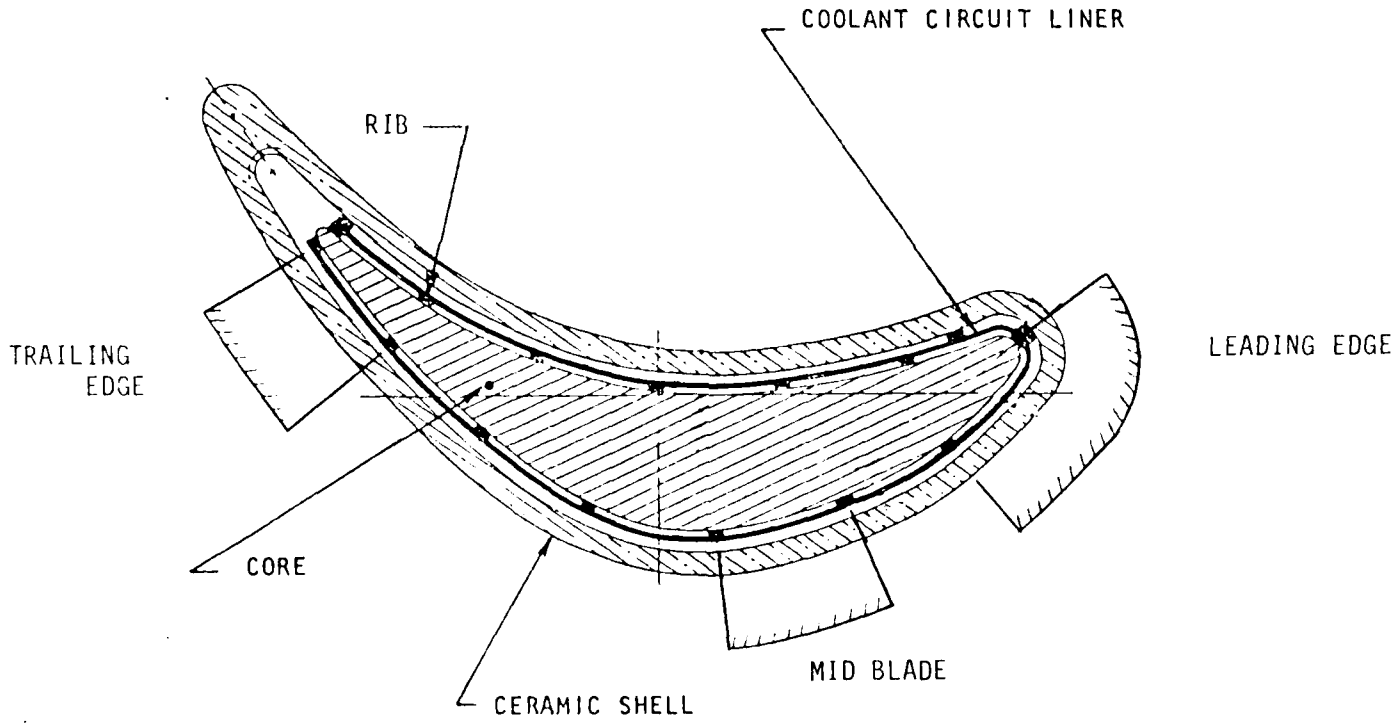

Figure 6
THERMAL ANALYSIS BLADE SECTIONS

THERMAL ANALYSIS
2-DIMENSIONAL FINITE ELEMENT MODEL

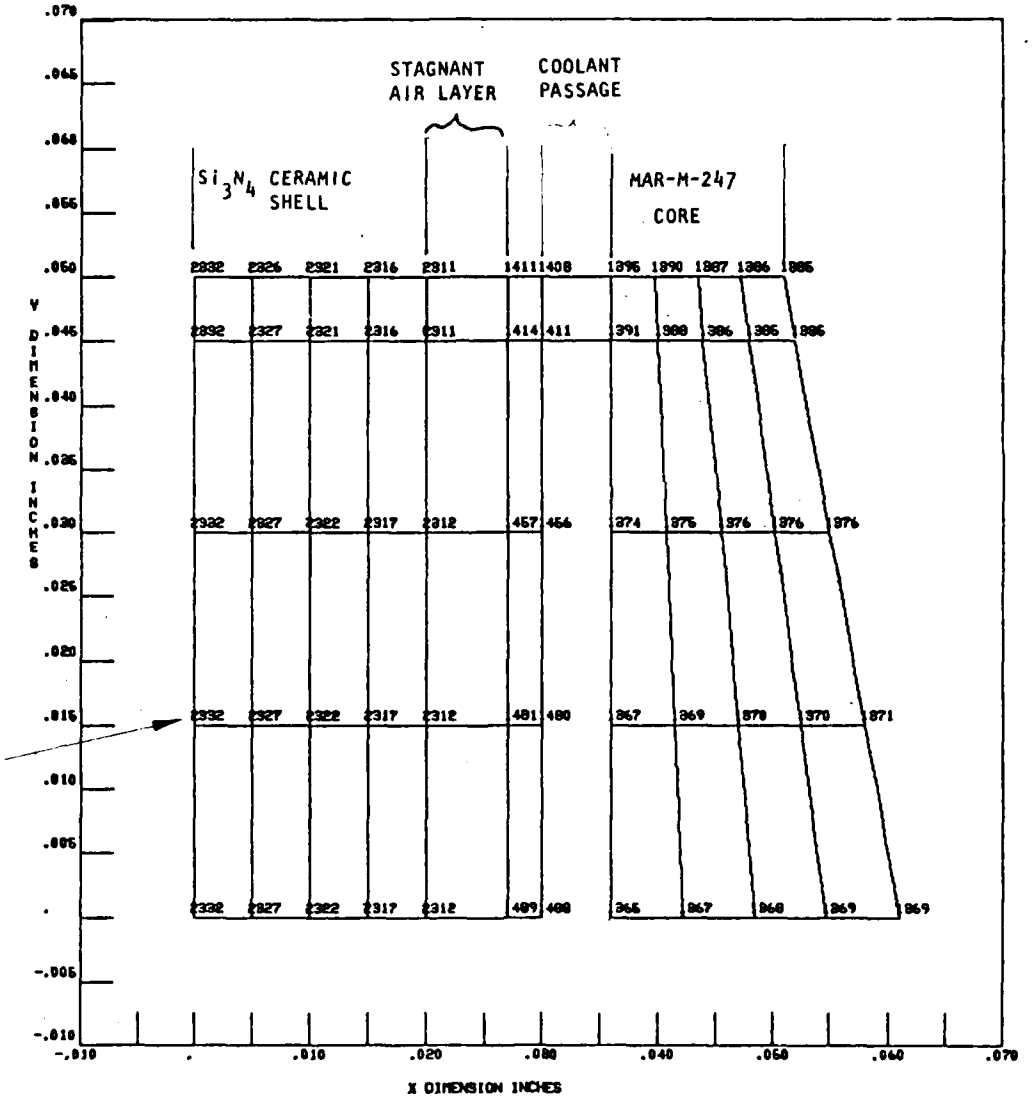

NODE IDENTIFICATION CALLOUT

FIGURE 7

The layered construction of the turbine blade optimizes the heat transfer mechanisms at the interfaces of each layer. Across the stagnant air gap, heat is transferred principally by conduction. A large temperature drop occurs across this gap due to the non-circulating air acting as an insulator. Cooling air flowing through the inner zone absorbs the little heat that crosses the stagnant air gap. Because heat transfer in this layer is by convection, most of the heat is carried away by the coolant flow.

The analysis was performed using the following steady state conditions:

Turbine Inlet Temperature	2650 F
Gas Heat Transfer Coefficient	
Leading Edge	450 BTU/hr ft^2
Mid section	200 BTU/hr ft^2
Trailing Edge	175 BTU/hr ft^2
Cooling Air Temperature	500 F
Cooling Air Flowrate	0.00167 lbm/sec

The results of the analysis are shown in Table 2. In this table the maximum temperatures of each component at the tip of the blade are presented. Also included is the temperature of the coolant air at this location. Figure 8 shows the change in temperature across the blade at the leading edge location. The effectiveness of the stagnant air layer is clearly evident by the 850 F drop in temperature across this layer.

The 1.0% engine compressor air flowrate used as coolant was more than sufficient to keep the core below 1500 F. Additional analysis was performed to minimize the coolant flowrate requirements. Figure 9 shows the effect of changing the percent of coolant flowrate on the temperature of each blade section.

Based upon this analysis, only 0.6% of the compressor flowrate is required to keep a Ceramic Barrier Turbine bladed rotor at a safe operating temperature while operating in a 2650 F turbine engine. Increasing the coolant flowrate to the acceptable limit of the engine would permit operating at turbine inlet temperatures approaching 2900 F.

HEAT TRANSFER ANALYSIS

	LEADING EDGE	MAXIMUM THICKNESS	TRAILING EDGE
• MAXIMUM SILICON NITRIDE BLADE SHELL TEMP (F)	2335	2135	2090
• MAXIMUM L-605 COOLANT LINER TEMP (F)	1490	1350	1320
• MAXIMUM MAR-M-247 BLADE CORE TEMP (F)	1395	1265	1240
• COOLANT TEMP (F)	1070	985	965

TABLE 2

TYPICAL TEMPERATURE DISTRIBUTION

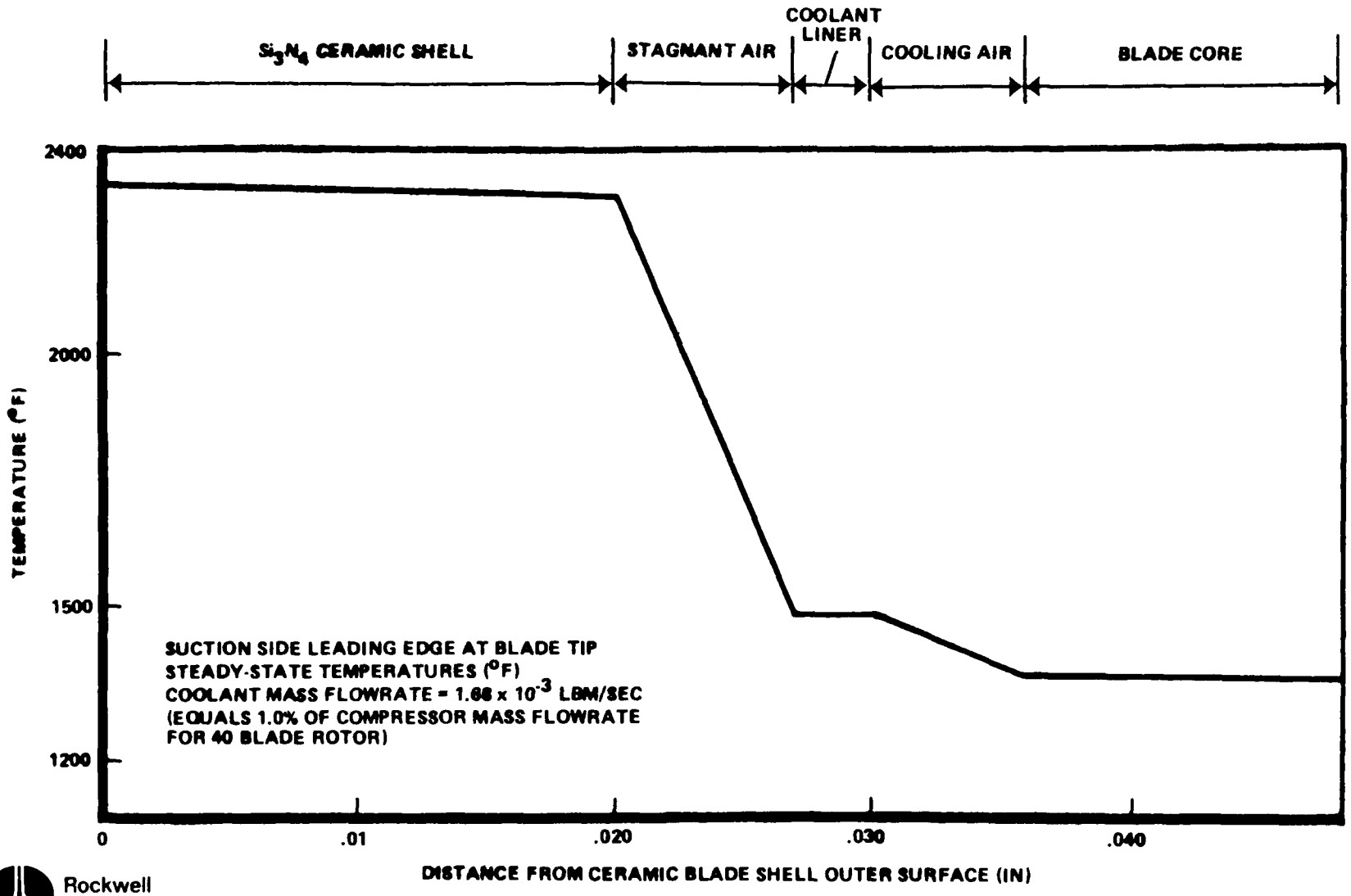

Rockwell International
Rocketdyne Division

FIGURE 8

COOLANT FLOWRATE REQUIREMENTS

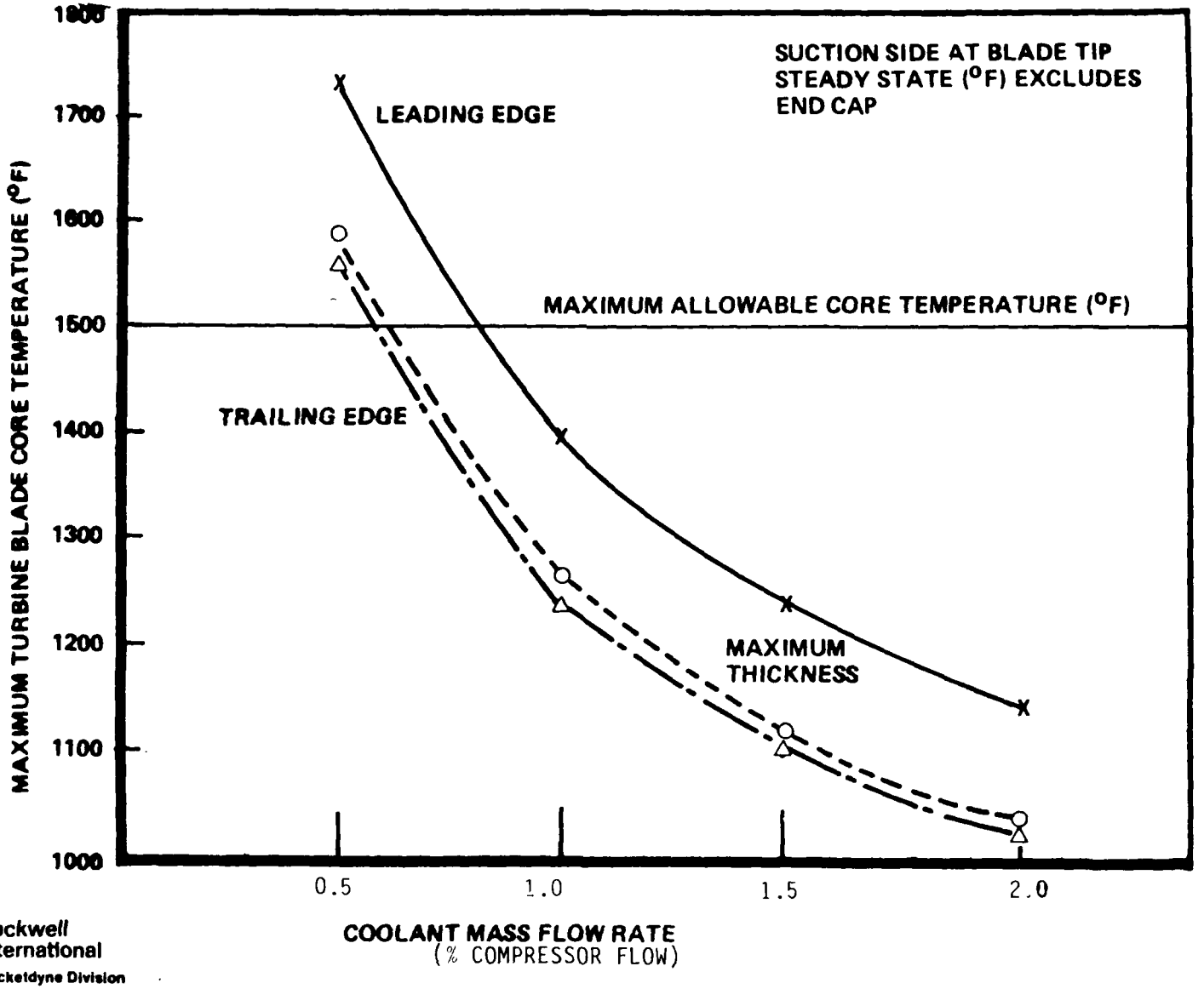

Rockwell International
Rocketdyne Division

FIGURE 9

STRUCTURAL ANALYSIS

The purpose of the structural analysis was to verify the structural integrity of each of the components of the Ceramic Barrier Turbine Blade. This included a probability of survival analysis for the shell.

Structural analysis was performed using finite element analysis modeling of each of the major blade components. These included the ceramic shell, the integral core and end cap, the coolant liner, and the footing. Each of the components were evaluated under thermal and centrifugal loading. Initial analyses were performed to support the iterative design effort. After finalization of the design, three dimensional models were constructed. The analysis used the ANSYS 3-D solution program.

The analyses were conducted using a steady state 57,000 rpm engine speed. Other conditions held constant were those associated with temperature (material strength and expansion). The material strengths for each component were based upon their material properties at their maximum temperatures determined during the thermal analysis (i.e. core at 1500 F, cap at 1800 F, etc). The physical properties for the silicon nitride were determined by Rocketdyne testing of the flexural and compressive strengths. The Weibull Modulus for each condition was also determined. These values are shown in Table 3.

TABLE 3 SILICON NITRIDE PHYSICAL PROPERTIES

Loading	Strength	Weibull Modulus
Flexural	76.2 ksi	13
Compressive	152.4 ksi * (388.0 ksi)**	12

* Southwest Research Institute Test Data
** Rocketdyne Test Data

The analysis included the effects of thermal growth at the interface of the ceramic with the end cap. This analysis was a two step process. First, the ceramic shell was assumed to be seated against the end cap under centrifugal loading at ambient temperature. The thermal growth effect was then added. The displacement of the end cap elements was greater than those of the ceramic shell, creating loading at the end of the shell. A non-deforming friction reducing layer was assumed to separate the two components.

The results of the analysis indicate all components would safely survive the operating conditions listed. The areas identified as having principal stresses are the loaded end of the ceramic shell, the trailing edge of the end cap, the base of the metal core, and braze joint of the footing. The magnitude

of the stress in each of these areas is shown in Table 4. Included is the factor of safety for each component based upon the elevated temperature material strengths.

The analysis indicated the trailing edge of the end cap will deflect due to its own weight and will pull away from the ceramic shell. The trailing edge of the shell will be left unsupported. This results in the transferring of the trailing edge weight to the adjacent sections. The stress in this section is more than twice the stress at other locations of the shell.

The probability of survival against rapid fracture of the ceramic shell was computed based upon the calculated Weibull values. A Weibull two parameter equation was used. The results are:

	Tension	Compression	Total
Probability of Survival	99.5%	99.9%	99.5%

PRODUCIBILITY

The Ceramic Barrier Turbine Blade was designed to use high volume production methods that would minimize fabrication costs. Proven materials such as MAR-M-246 and alloy 718 were selected. Machining is reduced by using cast components and sheet materials. The number of finished surfaces is minimal compared to equivalent cooled turbine blades. The number of precision machined surfaces are limited to the shell cap interface, the coolant exhaust holes, and footing profile. The material and fabrication requirements for the Ceramic Barrier Turbine Blade are shown in Table 5

TABLE 5 MATERIAL SELECTION

ITEM	MATERIAL	PROCESSING
Ceramic Shell	SN-205 Silicon Nitride (Si_3N_4)	Injection molded and sintered
Core/End Cap	MAR-M-246	Cast, finished machined
Coolant Liner	Alloy 718	Photoetched sheet
Friction Reducing	Haynes 25	Stamp pressed sheet
Locating Tabs	Alloy 718	Stamp pressed sheet
Wave Flexure	Alloy 718	Stamp pressed sheet
Footing	MAR-M-246	Electro-discharge machined

STRESS ANALYSIS SUMMARY

- **TWO ANALYSIS METHODS**
  - HAND ANALYSIS TO SUPPORT INITIAL BLADE DESIGN
  - 3D FINITE ELEMENT ANALYSIS TO DETERMINE STRESS DISTRIBUTION

AREA	TYPE OF LOAD	STRESS	F.S.
• TIP OF CERAMIC SHELL	COMPRESSION	21.0 KSI	19.0
• BASE OF CORE	TENSION	80.4 KSI	1.62
• FOOTING BRAZE JOINT	SHEAR	20.5 KSI	3.66
• CAP, TRAILING EDGE (CANTILEVER)	BENDING	74.0 KSI	1.76

- **ALL PRINCIPLE STRESS AREAS ABOVE MINIMUM FACTOR OF SAFETY (1.4)**

TABLE 4

Silicon nitride was selected for its high strength and thermal shock resistance. The material is a proprietary Rocketdyne developed composition in which yttria (Y_2O_3) and silica (SiO_2) are added as sintering aids. The shells are formed using the injection molding process. Machining is limited to grinding of the two ends to make them flat and parallel. This grinding operation is controlled to prevent development of a subsurface distressed condition.

The core/end cap and footing are made from cast MAR-M-246. Casting of these parts will produce surfaces with sufficient accuracy that additional machining of the profile is not required. The seating surface for the ceramic shell is machined to provide a smooth surface. The supply and exhaust cooling holes are added by EDM drilling. The profile of the footing halves where they are brazed onto the core are wire EDM'd. The footing and core are kept oversized for incorporating alignment pins and clamping surfaces.

The coolant liner is made by photoetching the coolant passages into one side of a sheet of 0.009 inches thick alloy 718. Several parts would be etched and trimmed from a single large sheet to reduce handling costs. The locating tabs are brazed onto the coolant liner while they are part of the large sheet.

The friction reducing layer and wave flexure components would be stamp pressed from flat sheets of Haynes 25 or alloy 718, respectively. For the wave flexure, the cutting die would have a corrugated shape to form the wavey surface of the flexure.

All of the components are finished machined prior to assembly (the footing receives additional machining after assembly). Each component is inspected to ensure its integrity prior to approving it for assembly. All of the metal components are inspected using standard, nondestructive inspection methods.

Non-destructive inspection techniques are not capable of reliably locating all of the subsurface defects in ceramic materials. Since it is important to cull the defective parts, the ceramic shells undergo a pass or fail proof test. The proof test will be a centrifugal spin test because standard two sided compression testing would not simulate actual, operational-induced stresses.

The sequence for assembling the blade is shown in Figure 10. The coolant liner is first brazed to the core by wrapping it around the leading edge. Any small dimensional differences between the two parts is accommodated at the trailing edge. A holding fixture maintains the correct position during brazing. All brazed surfaces are nickel plated to improved bonding.

The friction reducing layer and the ceramic shell are installed by slipping them over the base of the core. Neither of these components are bonded or rigidly held in place. A twisted blade profile can be accommodated by this assembly method provide the twist is at a constant rate.

ASSEMBLY SEQUENCE

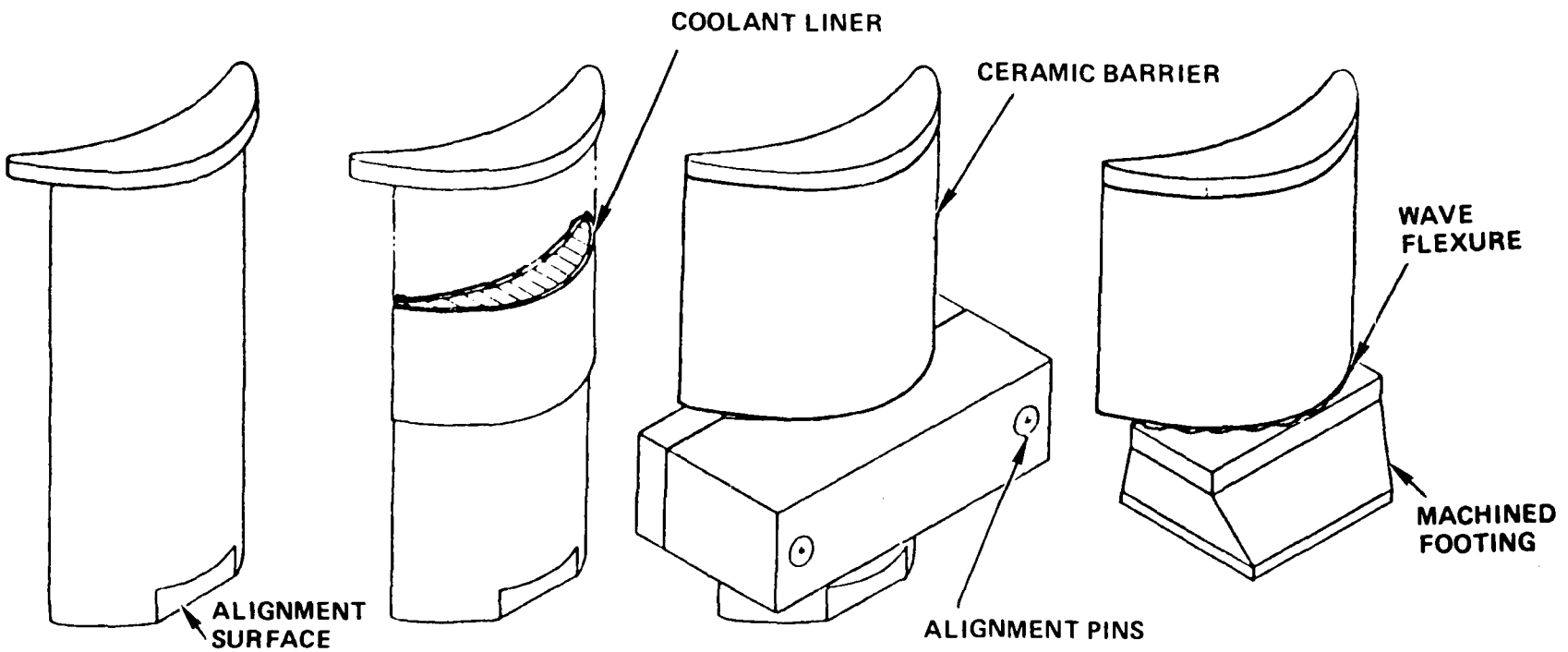

1. INTEGRAL CORE/CAP
2. COOLANT LINER INSTALLED
3. CERAMIC BARRIER, FRICTION REDUCING WASHER, FOOTING INSTALLED
4. FOOTING MACHINED, WAVE FLEXTURE INSTALLED

487-603A

Rockwell International
Rocketdyne Division

FIGURE 10

CORE/FOOTING ASSEMBLY CONCEPT

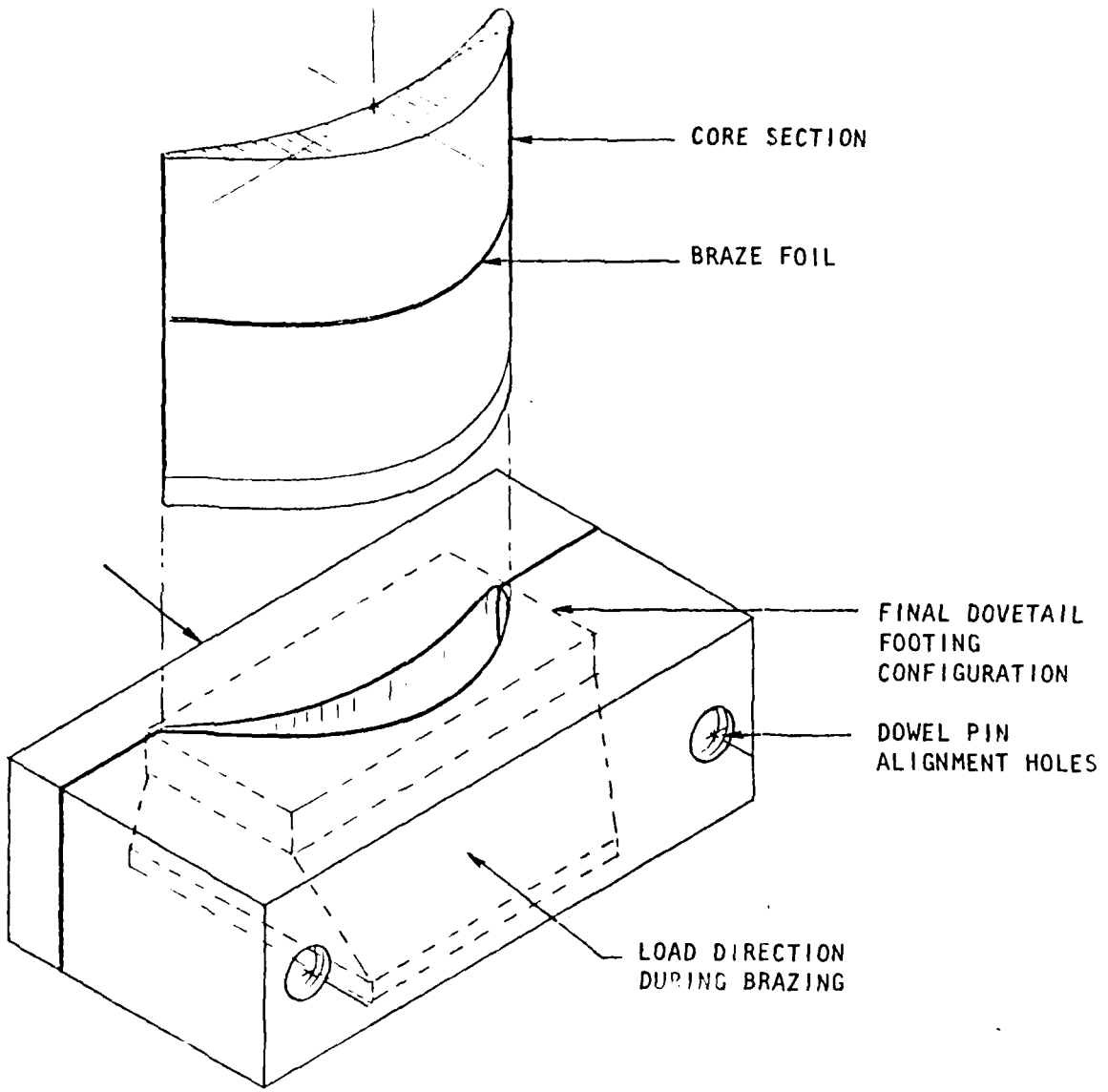

FIGURE 11

The oversized footing halves are next assembled around the base of the core. The core and footing are made oversized to incorporate the use of alignment surfaces and pins as well as clamping surfaces, shown in Figure 11. These components are joined together by brazing. The large surface area of this joint ensures a strong bond. The ceramic shell is not affected by either the braze cycle temperatures or the aging heat treatment required to restore the MAR-M-246 material strength.

The final configuration of the footing is then wire EDM'd. The ceramic shell is not affected by the EDM process. The footing profile can be either a firtree configuration for production installations or a dovetail, like the one shown in these figures, used for development testing. The final step in blade assembly is insertion of the wave flexure.

HARDWARE FABRICATION

Production of the metal components, the core, coolant liner, and footing, are straightforward and do not present a development risk. The ceramic barrier was identified to require fabrication development. Design and procurement of the injection mold die and production of several shells for spin testing comprised this fabrication task. This section details the development of the shell fabrication process.

MATERIAL PREPARATION

A proprietary SN-205 silicon nitride material developed at Rocketdyne was used for molding of the airfoil specimens. The silicon nitride powder is combined with binders and sintering aids and a plastizier is added to act as a carrier vehicle for injection molding. After molding, the binder and plastizer are removed. The parts are then sintered to full density. Figure 12 shows the airfoil specimens after each step in the process. There is an approximate 50% reduction in volume of the part from the injection molded state to the final condition.

Heat treatment and HIP'g the sintered parts increases both the tensile and compressive strengths. These additional steps were not necessary for the components produced for this program.

INJECTION MOLDING

A mold was designed and fabricated for forming the airfoil specimens. A major unknown in fabrication of the airfoil specimens was how the plastizied silicon nitride would flow through thin cavity sections. The walls of the finished ceramic shell varies from 0.015 to 0.020 inches in thickness. The wall separation at the thinner sections of the mold, which include the shrinkage factor, is 0.024 inches.

The mold die was developed for producing the silicon nitride airfoil shells to the net profile. In addition to producing airfoil specimens that met dimensional requirements, the mold die design would channel the material flow to minimize weld lines and the gate would be remotely located away from the finished part. Previous experience found subsurface blemishes form near the mold gate.

The flow characteristics of silicon nitride through the mold is to fill areas of least resistance, i.e. the wider sections first. For this reason, a reservoir feed system was used. A large cavity is added over one end of the blade cavity. On either side of the reservoir are the inlet gates. Material fills the reservoir first, then fills the blade in one smooth flow.

The sequence of material flow through the mold, shown in Figure 13, is illustrated by a series of "short shots". Because the airfoil specimen trailing edge has the least resistance, this area fills first. What was unusual was that the remaining blade sections filled from the smaller

FIGURE 12

SILICON NITRIDE AIRFOIL
TEST SPECIMENS

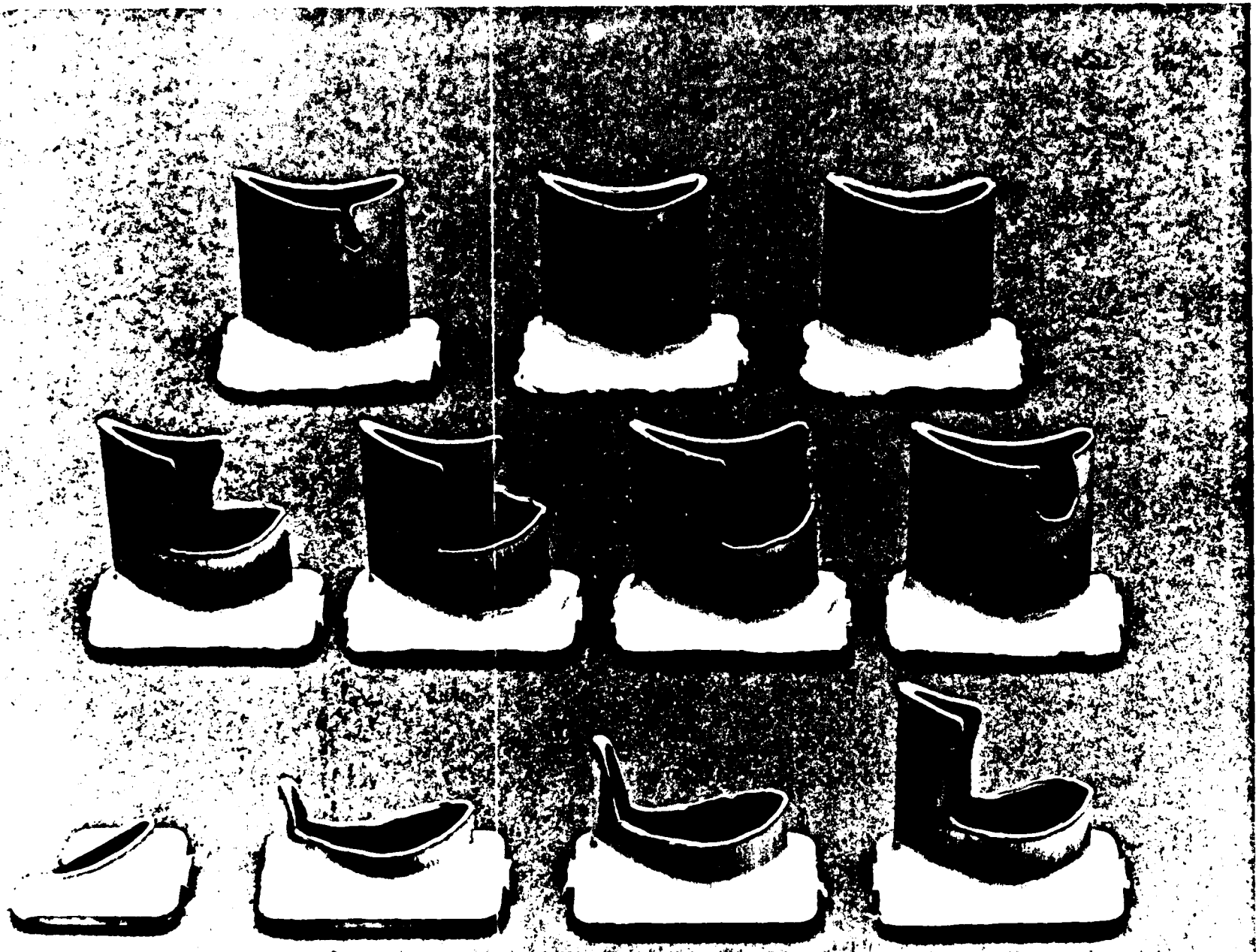

FIGURE 13

CAVITY FLOW PATTERN

reservoir formed by the trailing edge rather than the larger main reservoir. The material would flow forward around the core piece and meet at the leading edge. This would result in a weld line in a high stress area.

Another problem with this flow pattern was that the pressure side cavities filled faster than the suction side cavities. A force was exerted by the material on the core causing it to bend towards the suction side. These problems were reduced to an acceptable level by reworking of the mold and adjusting of the molding parameters.

Twenty-four (24) airfoil shells were processed through the sintering stage. Of these, thirteen (13) were available for testing. The other eleven shells were damaged either during grinding or found to have small surface blemishes uncovered during grinding. A summary of the dimensional inspection results is presented in Table 6 and a sample airfoil shell is shown in Figure 14. This inspection proved that silicon nitride components produced by injection molding have repeatable and acceptable tolerance variations.

TABLE 6 SILICON NITRIDE AIRFOIL SHELL

FINISHED DIMENSIONS

FEATURE	DESIGN DIMENSION	ACTUAL DIMENSION	MEASURED TOTAL DEVIATION
CHORD LENGTH in.	0.720	0.720	0.023
BLADE HEIGHT in.	0.715	0.600 *	CONTROLLED BY GRINDING
BLADE WEIGHT gr.	---	1.011	0.026
WALL THICKNESS in.			
PRESSURE SIDE, HUB	0.015	0.023	0.004
SUCTION SIDE, HUB	0.015	0.015	0.003
PRESSURE SIDE, TIP	0.020	0.022	0.004
PRESSURE SIDE, TIP	0.020	0.016	0.006

* Length reduced during mold rework

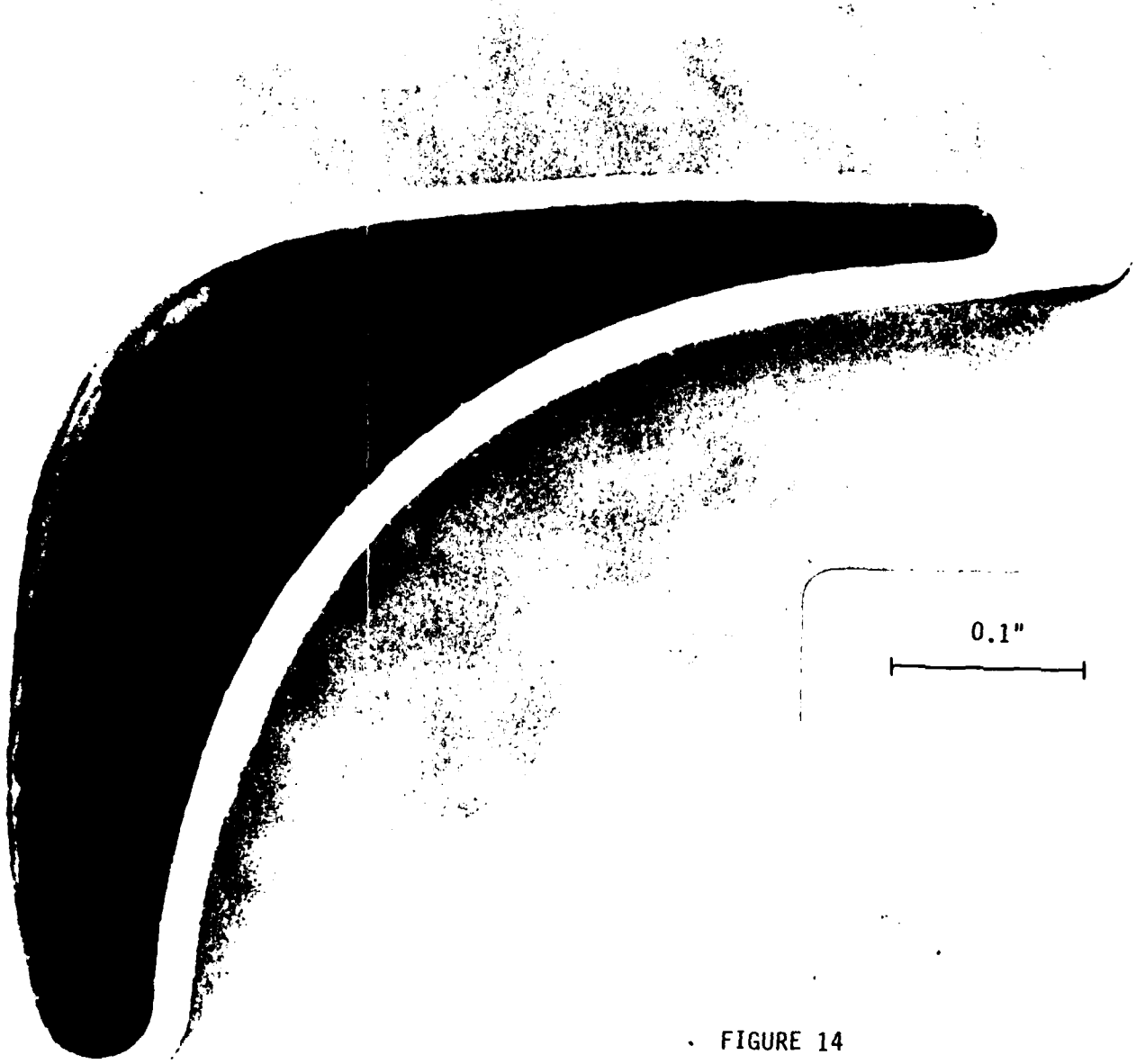

FIGURE 14

AIRFOIL SPECIMEN

PROFILE
BLADE #18

TEST

Spin testing of the airfoil shells was performed to verify their structural integrity as predicted by stress analysis. This proof test would also determine if the fabrication process for making the shells had introduced defects that could lower the strength of the part. In addition to spin testing of the airfoil shells, testing was conducted using ceramic cylinder specimens. The simple shape of the cylinder would result in uniform compressive loading. The spin test duplicates shell loading due to centrifugal forces during engine operation.

SPIN TEST FACILITY

Testing was performed in the vertical vacuum spin pit in the Rocketdyne Engineering Development Laboratory. The test rotor is suspended by a quill shaft (Figure 15) and is driven by a two inch gaseous nitrogen turbine up to 66,000 rpm. A catcher assembly with nylon inserts is installed below the rotor (Figure 16) to prevent damage to the rotor should the quill shaft fail.

All testing is performed in a vacuum (at ambient temperature) to eliminate the development of aerodynamic forces that might act to displace the rotor. The position and stability of the rotor is monitored using a set of proximity transducers spaced 90 degrees apart. The displacement redline for the rotor was set at 0.005 inches. For all tests, the rotor was balanced to within 0.02 gram-inches.

CYLINDER SPIN TESTING

A series of spin tests using cylinder specimens were conducted to establish baseline performance of the silicon nitride material. The geometry of the specimen was a simple right cylinder (Figure 17). The rotor and support studs (Figures 18 and 19) retain the specimens in a manner similar to the way the shells are retained in the Ceramic Barrier Turbine Blade. This test setup results in single sided compressive loading of the cylinder. Haynes 25 washers were inserted between the ceramic cylinder and support studs for selected tests to establish baseline performance for this material.

Of the sixteen cylinder specimens tested, fourteen (14) or 88% of the pieces survived the spin test. The results of the tests are summarized in Table 7. No problems were found in these samples after post test inspection. A inspection of the Haynes 25 washers found no indications of surface deformation, qualifing this material for further testing.

Two of cylinder specimens had cracked during the test. In cylinder #29, there was a single crack running the length of the cylinder. In cylinder #9, a 90 degree section of the cylinder had separated, (Figure 20). The separated section did not fly off of the stud and was recovered. These specimens had been inspected prior to the second spin and no cracks were found at that time.

Microscopic examination of the failed specimens was unable to locate the failure initiation point. The cracks of both cylinders were similar in that

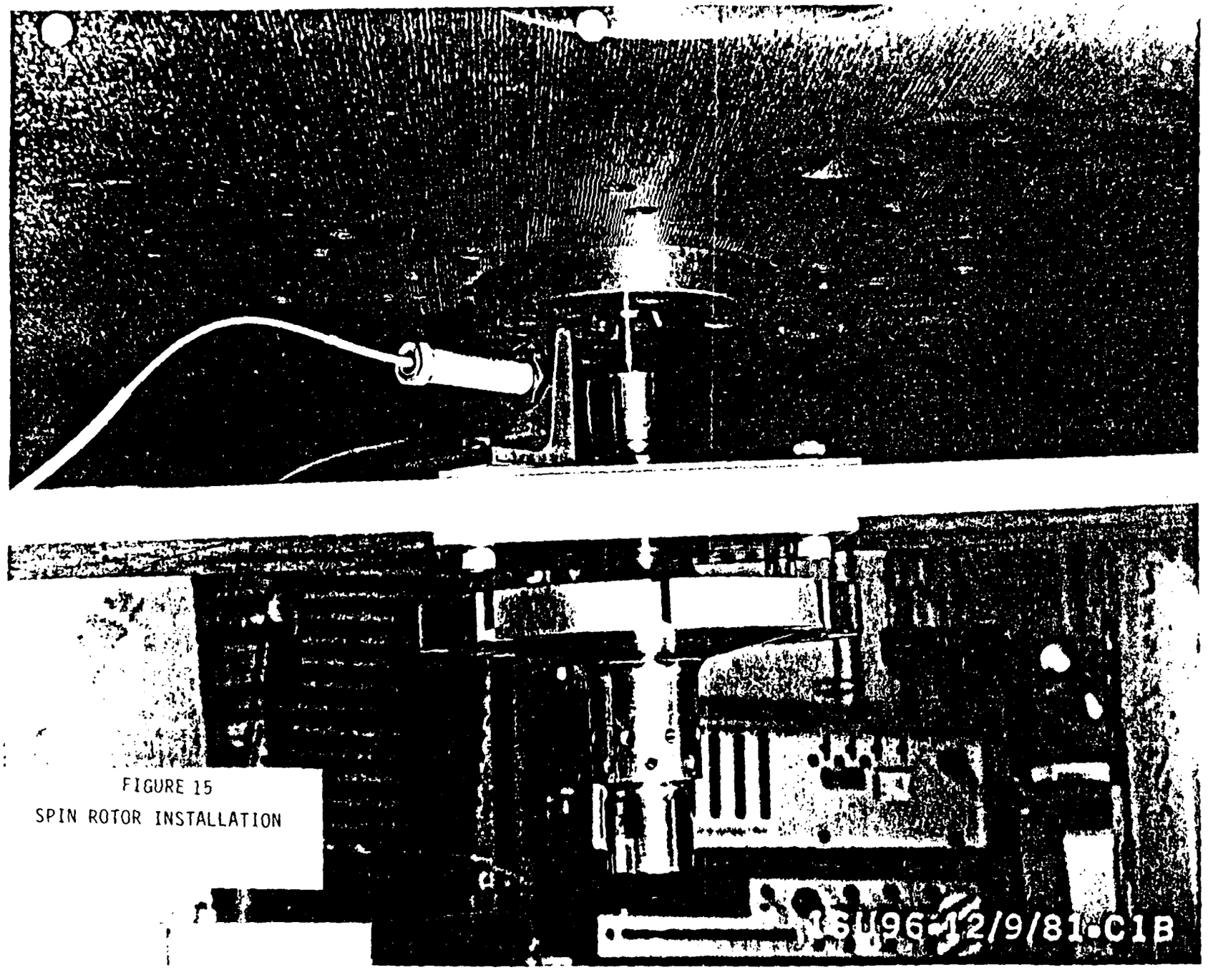

FIGURE 15
SPIN ROTOR INSTALLATION

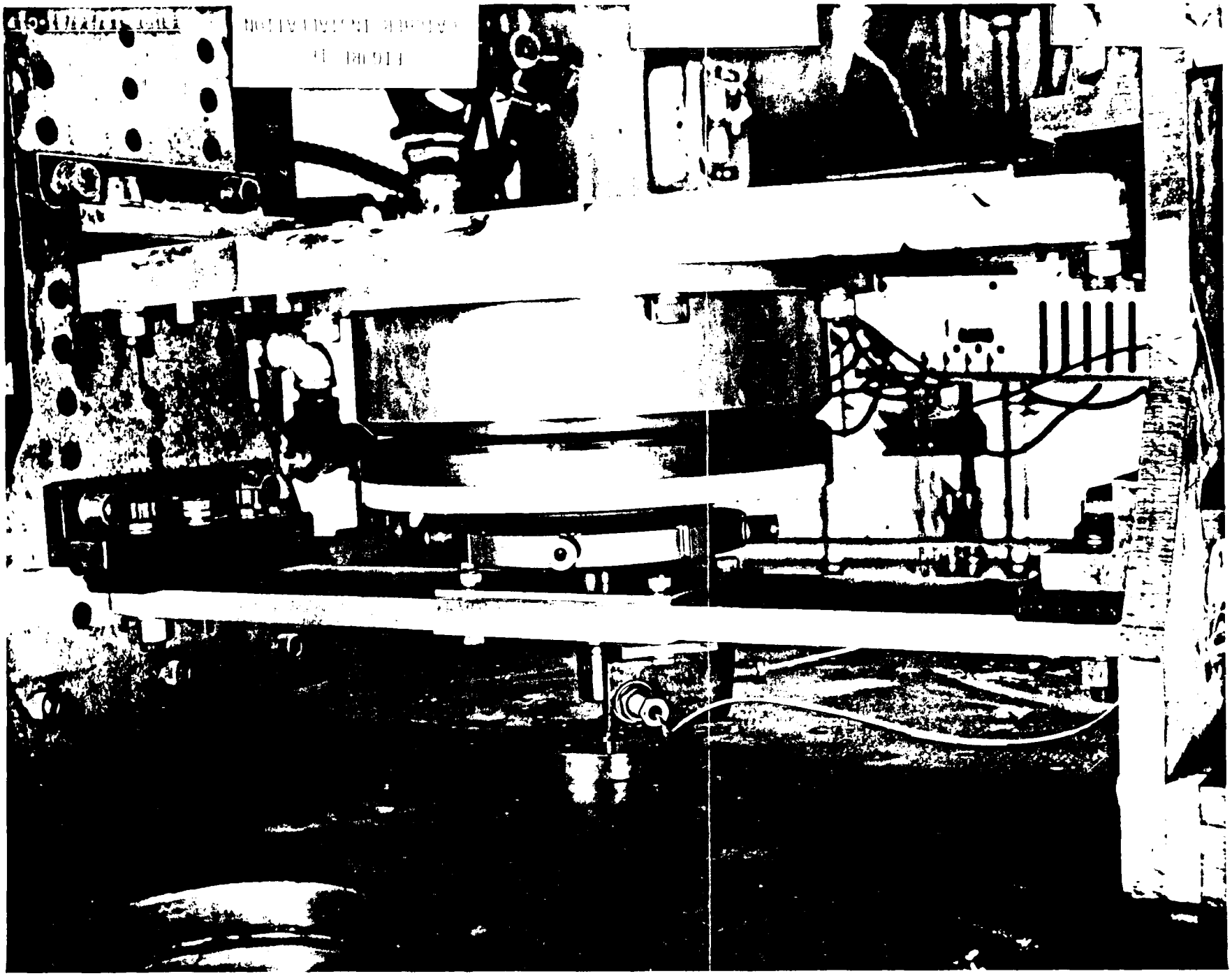

COMPRESSIVE TEST SPECIMEN

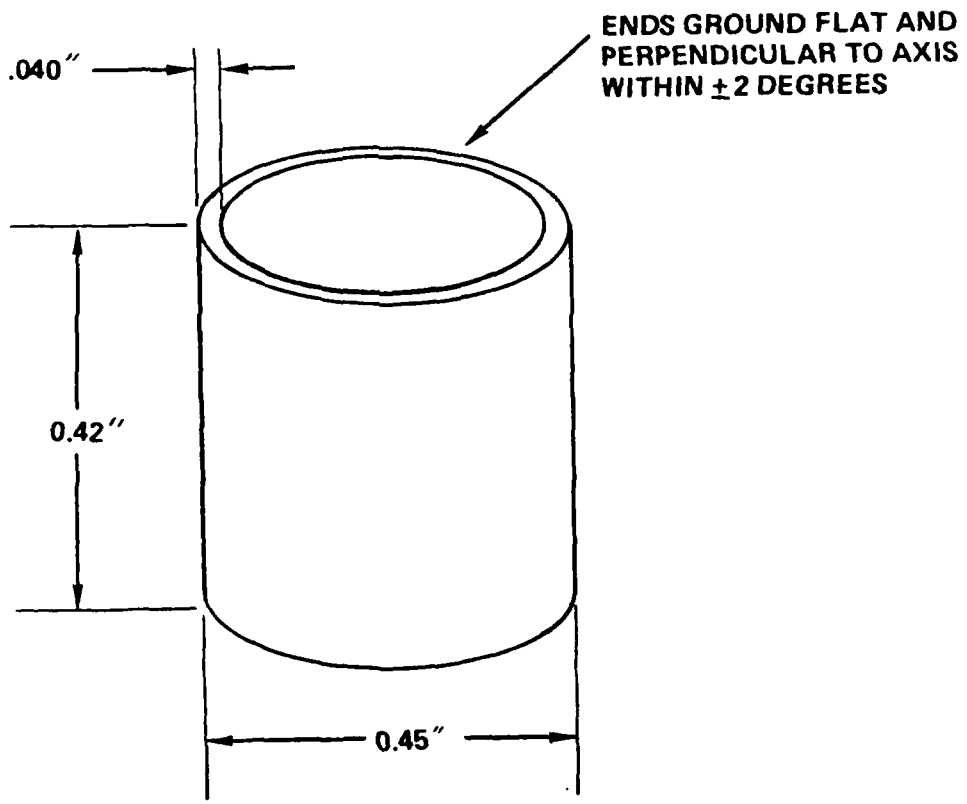

FIGURE 17

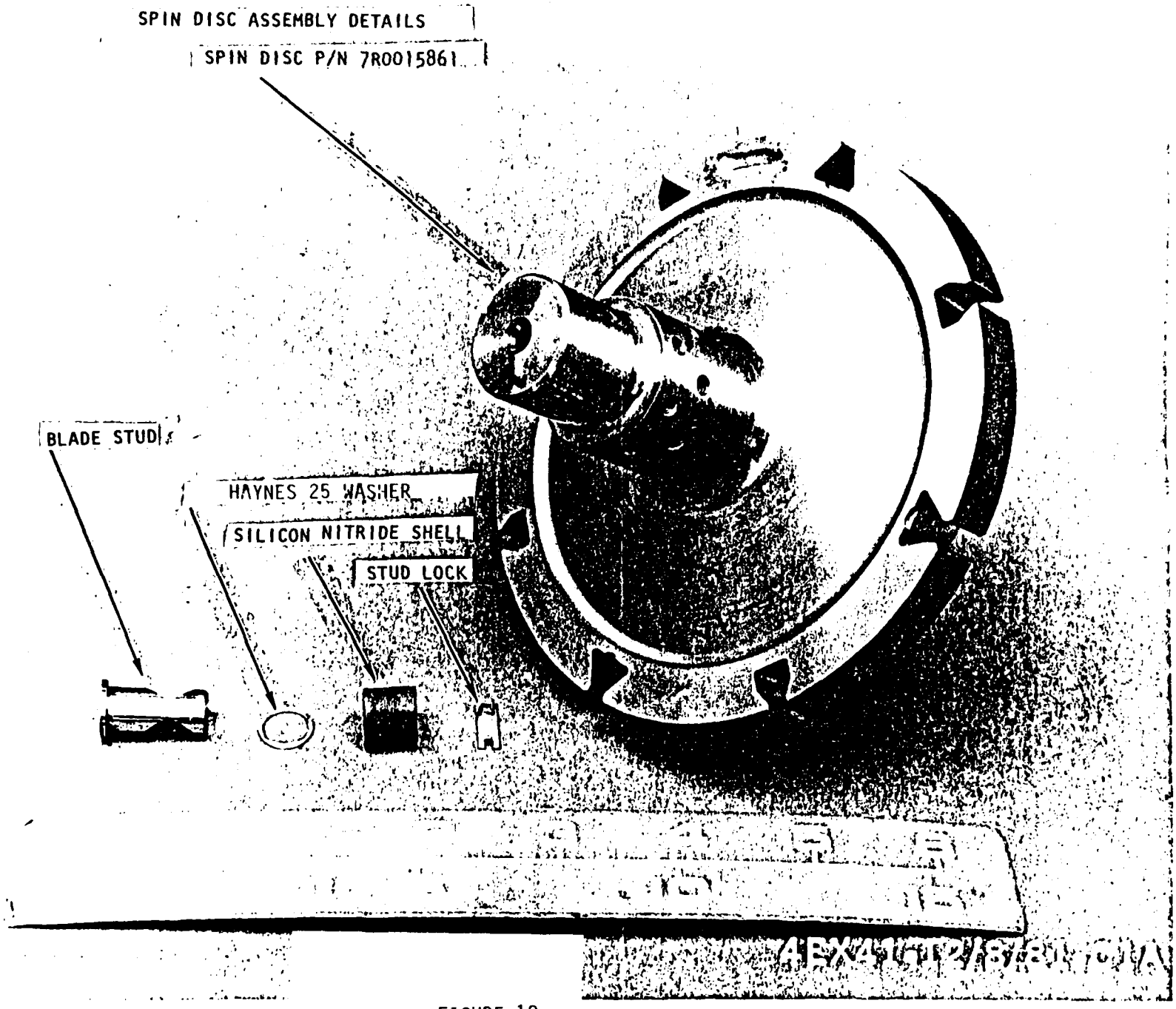
SPIN DISC ASSEMBLY DETAILS
SPIN DISC P/N 7R0015861
BLADE STUD
HAYNES 25 WASHER
SILICON NITRIDE SHELL
STUD LOCK

FIGURE 18

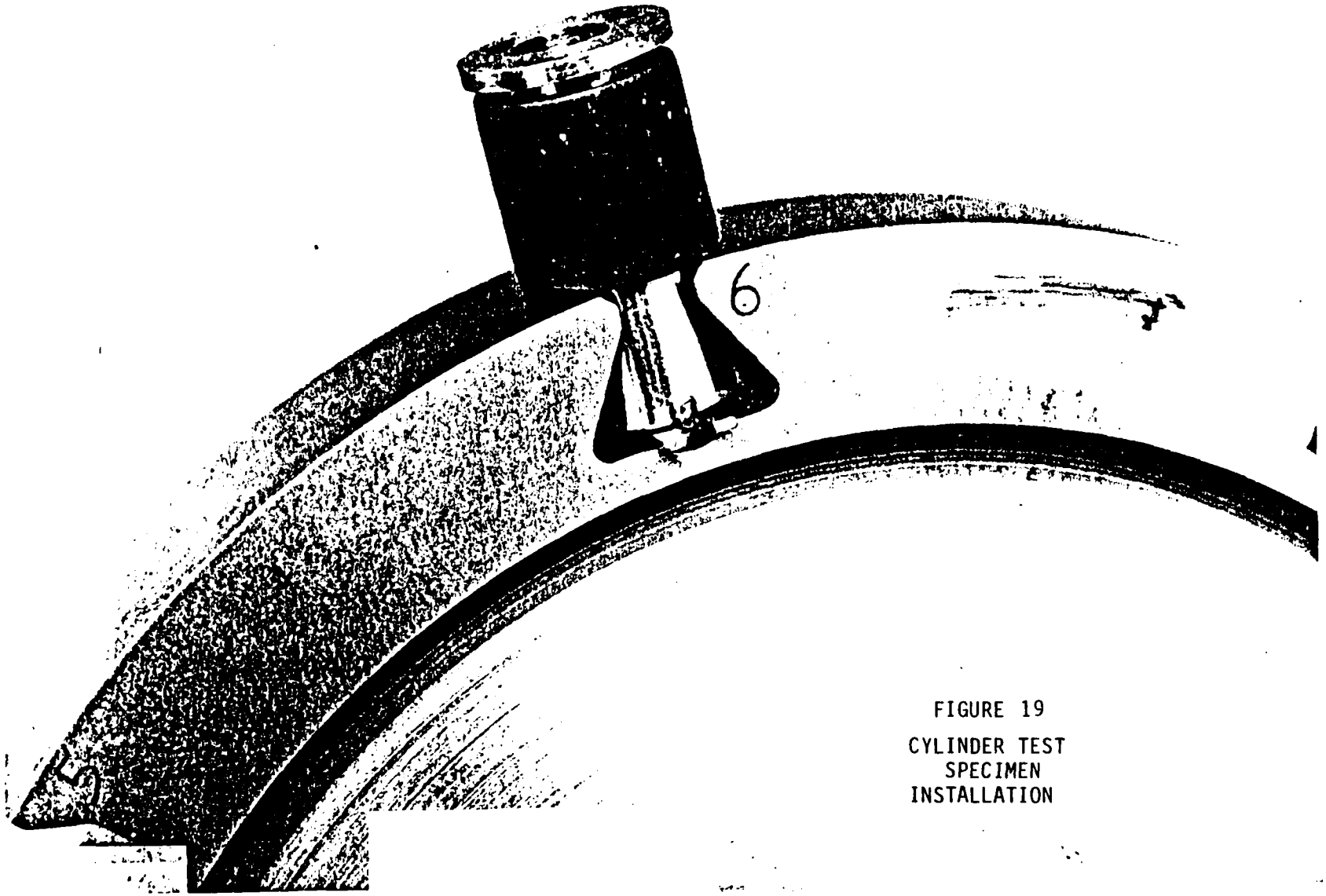

FIGURE 19

CYLINDER TEST
SPECIMEN
INSTALLATION

TABLE 7 SPIN TEST RESULTS

SILICON NITRIDE CYLINDERS

TEST	SPEED (RPM)	DURATION (MIN)	CENTRIFUGAL LOADING (KSI)	SPECIMEN SERIAL NUMBER	PRETEST VISUAL BLEMISH	COMMENTS
A	59,500	2.5	15.8	23	NO	PASSED
				41	YES	PASSED
				19	YES	PASSED
				68	NO	PASSED
B1	59,900	2.5	16.1	44	NO	PASSED
				9	NO	CRACKED, SUBSURFACE DEFECT
B2 *	59,900	2.5	16.1	18	YES	PASSED
				69	YES	PASSED
C	58,000	0.2	14.9	29	NO	CRACKED, SUBSURFACE DEFECT
				46	NO	PASSED
				51	NO	PASSED
				40	NO	PASSED
D	60,000	1.5	19.4	49	YES	HAYNES 25 WASHER, PASSED
				33	YES	HAYNES 25 WASHER, PASSED
	66,000 **	1.5		16	YES	HAYNES 25 WASHER, PASSED
				47	YES	HAYNES 25 WASHER, PASSED

* BACK-TO-BACK TEST

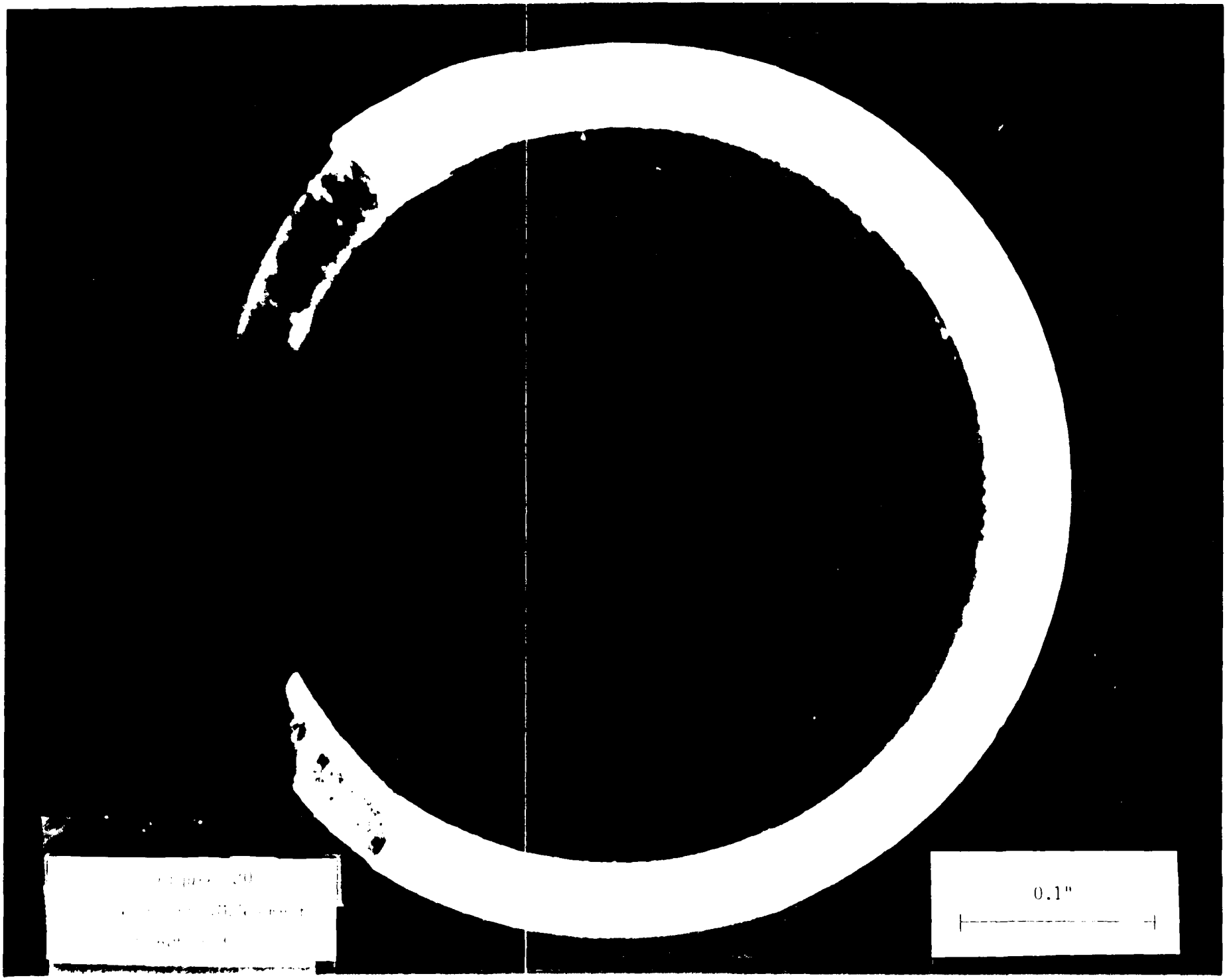
0.1"

they both ran through identical areas on either side of the injection mold gate. Of the specimens tested, 56% had a small surface blemish in this location, (Figure 21). These defects were subsurface defects that were uncovered during grinding. Their appearance is similar to a cold shunt found in metal castings. They formed during injection molding and enlarged during sintering. No other defects had been found on any other surfaces of the cylinders.

It was determined that an undetected defect, associated with the mold gate, contributed to the failure of the two cylinders. As a result, the specifications for the airfoil shell injection mold die required that the mold gate be remotely located from the finished part.

Several test attempts were terminated before reaching the target speed when the rotor displacement exceeded the redline limit of 0.005 inches. This rotor had been used during a prior test program, being spun to 66,000 rpm for five (5) tests without incident. A modification was made to the rotor and the first test stayed within the displacement limits. Further testing achieved a speed of only 23,000 rpm before reaching the redline limit and the test terminated. No further effort was expended on testing the cylinders because the baseline material characteristics had been established.

CERAMIC SPIN TEST

Ceramic shell spin tests were conducted using a new rotor specifically design for these components. The rotor and support studs, both made from alloy 718, are shown in Figure 22. Provision was made for testing six (6) specimens simultaneously. The diameter at the loaded end of the shell is the same as the engine rotor diameter (5.88 inches) so the test speed equalled the engine operating speed of 57,000 rpm.

A new type of reuseable mounting stud was used for retaining the ceramic shells. The mounting stud and airfoil specimen are shown in Figure 23. This stud has a half rounded section to adapt to the curvature of the rotor while providing a flat surface for the shell to seat against. Attached to the main stud is an airfoil shaped piece (called the positioner) that fits inside the airfoil shell (Refer to Figure 22). This inner piece maintains the correct shell position and prevents it from falling out of the pocket when the rotor is suspended on the quill shaft. A threaded pin retains the entire assembly in the rotor when it is suspended vertically. Two of the studs were modified to include a 0.011 inch layer of Haynes 25 material separating the ceramic and metal parts.

Thirteen (13) silicon nitride airfoil shells were proof tested in a series of three spin tests. The shells were brought up to speed in approximately one minute and held at the final speed for 2 1/2 minutes. The third test was run at an overspeed condition of 60,000 rpm. Two of the shells were installed for all three tests while one shell was used for two tests. A lubrication leak in the drive turbine prevented further testing.

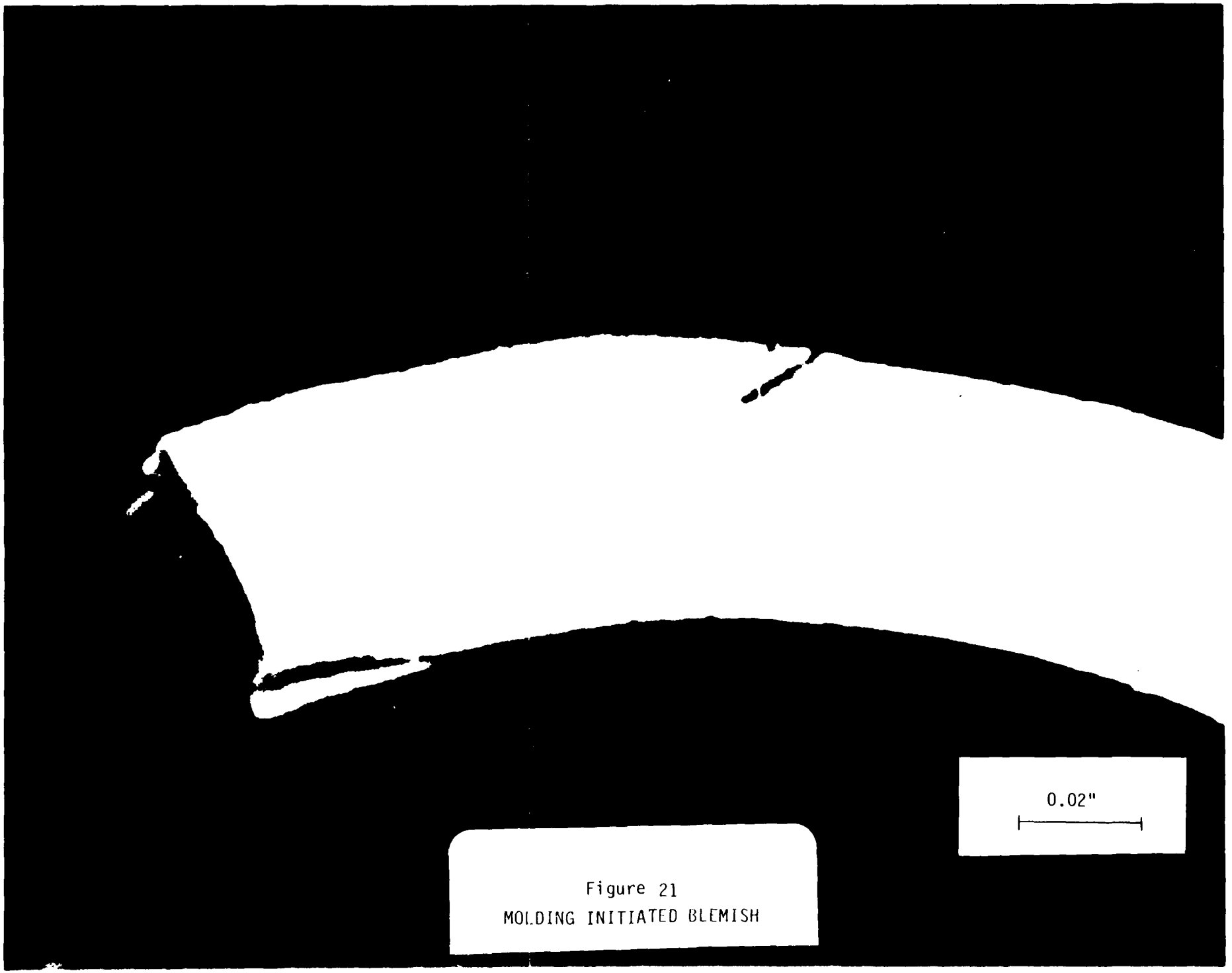

Figure 21
MOLDING INITIATED BLEMISH

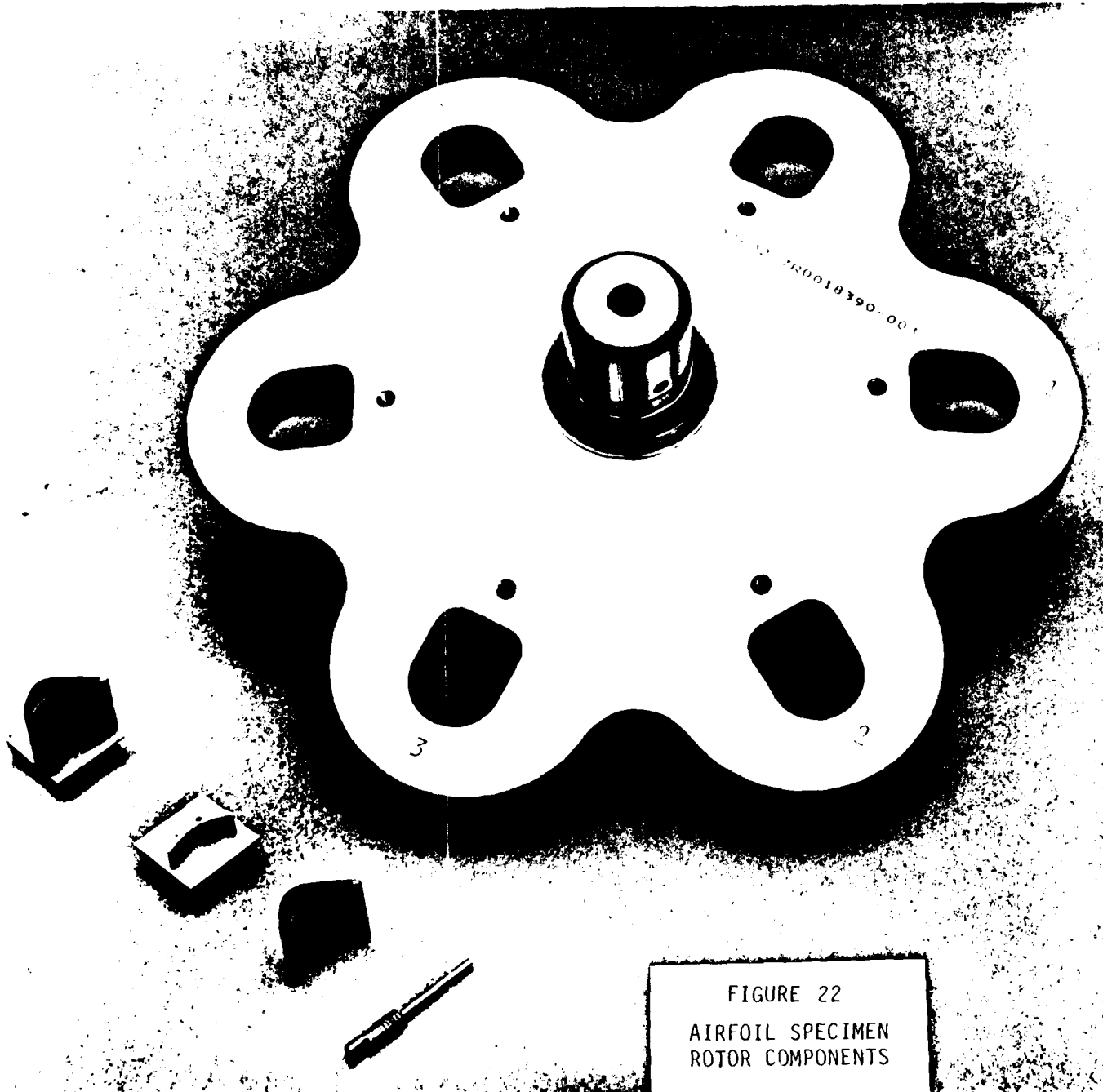

FIGURE 22

AIRFOIL SPECIMEN
ROTOR COMPONENTS

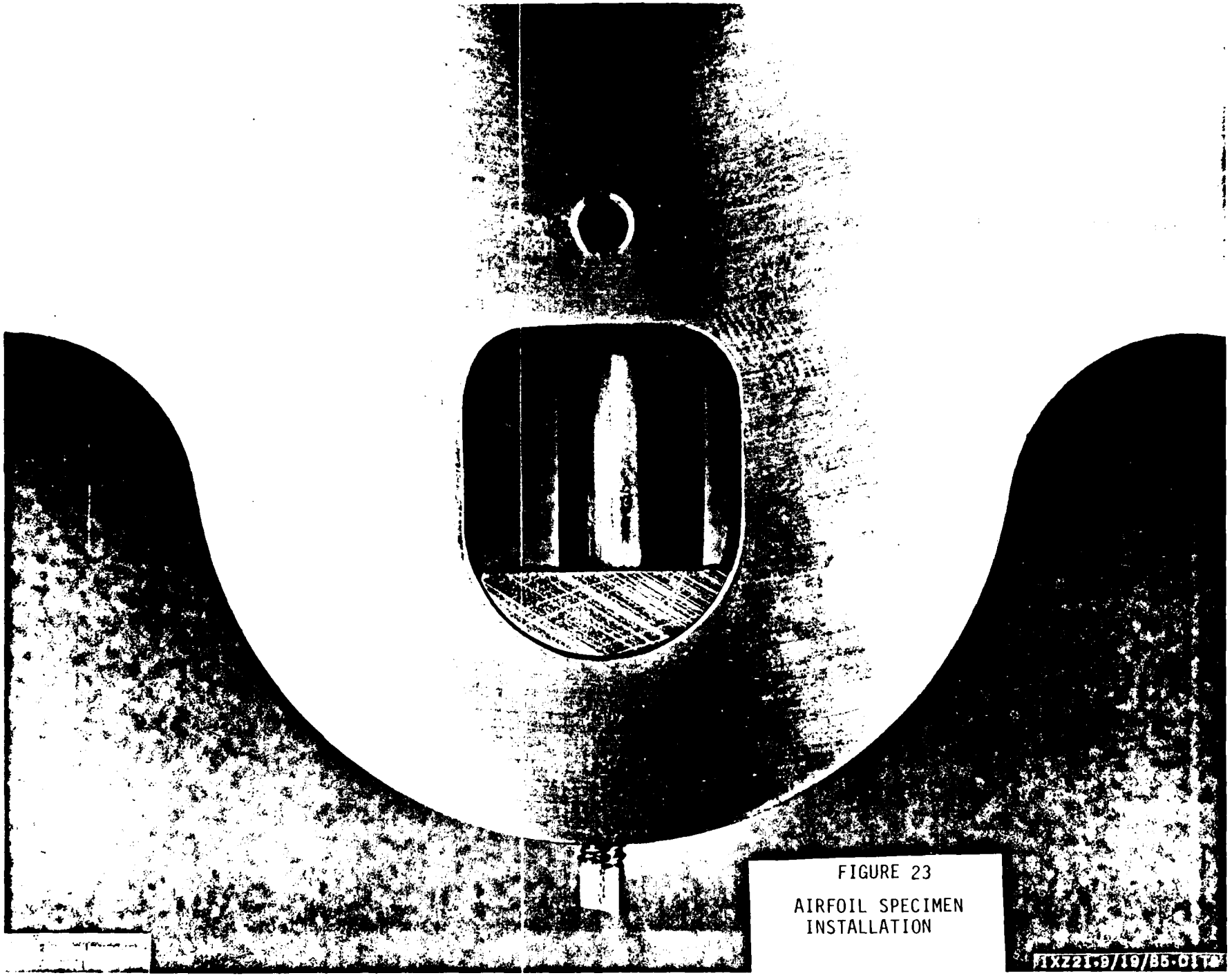

FIGURE 23

AIRFOIL SPECIMEN
INSTALLATION

All of the thirteen shells (100%) survived the spin test. The results of the tests are summarized in Table 8. Post test inspection using 50x magnification did not find any changes in the condition of the ceramic shells, the alloy 718 support studs, or the Haynes 25 friction reducing washers. All components performed as predicted. This test proved that complex (non-symetric), thin walled silicon nitride components are capable of surviving the single sided loading condition required by the Ceramic Barrier Turbine Blade design.

TABLE 8 SPIN TEST RESULTS

SILICON NITRIDE AIRFOIL SHELLS

TEST	SPEED (RPM)	DURATION (MIN)	CENTRIFUGAL LOAD (KSI)	AIRFOIL SERIAL NUMBER	COMMENTS
				5	PASSED
				2	PASSED
1	57,000	2.5	16.6	1	PASSED, HAYNES 25 WASHER
				13	PASSED
				3	PASSED
				4	PASSED, HAYNES 25 WASHER
				5	PASSED
				12	PASSED
2	57,000	2.5	16.6	14	PASSED, HAYNES 25 WASHER
				13	PASSED
				17	PASSED
				15	PASSED, HAYNES 25 WASHER
				5	PASSED
				7	PASSED
3	60,000 *	2.5	18.4	10	PASSED, HAYNES 25 WASHER
				13	PASSED
				8	PASSED
				15	PASSED, HAYNES 25 WASHER

* OVERSPEED CONDITION

CONCLUSIONS

This program analytically verifies the capability of the Ceramic Barrier Turbine Blade design to withstand the thermal and loading environment of the F107 turbine engine. The ability of the ceramic shell to withstand high centrifugal loads was experimentally verified.

It has been demonstrated that airfoil-shaped, thin-walled silicon nitride shells can be fabricated to withstand the forces imposed upon them during engine operation. Sample silicon nitride shells with walls only 0.015 inches thick were produced and ambient spin tested at simulated engine speeds. The spin test verified that the calculated load factor of safety of 19 and the 99.5% probability of survival would ensure a highly survivable, reliable component.

The production costs of the Ceramic Barrier Turbine will be low because all of the components can be fabricated using commonly available materials and production processes. Each component is fabricated separately and can be fully inspected or proof tested prior to accepting it for assembly. In addition to a lower scrap rate and cost, each finished blade assembly will be a highly reliable component that can be interchanged with any unit on the turbine rotor. This feature, and the fact that currently available test engines and facilities can be used without significant modification, is expected to present lower development costs over monolithic ceramic turbine blades.

The Ceramic Barrier Turbine Blade can be used for the next generation of turbine engines, being designed with operating temperatures around 2600 F as well as future engine developments with operating temperatures around 2900 F.

RECOMMENDATIONS

Based on the successful spin test of the Ceramic Barrier Turbine Blade shell, it is recommended that the development of this promising high temperature blade design be continued with verification of its thermal as well as loading capability. Complete blade assemblies should be fabricated and hot spin tested. The blade geometry and operating requirements shall be for an existing turbine engine such that transition to engine testing can be made. The program will be structured into three tasks: blade design and analysis, fabrication, and hot spin testing. Design effort shall include detailed design and analysis of the end cap with cooling passages and the firtree footing attachment. The fabrication effort shall produce several completed blades. Spin testing shall be performed in an existing hot spin component tester to validate the complete blade design. The tester shall be capable of simulating the temperatures and speeds at which the gas turbine will operate. The completion of this thorough blade qualification program will clear the turbine blade for follow-on testbed engine testing.

DISTRIBUTION LIST

Copies

2 Commander, Defense Technical Information Center, Cameron Station, Building 5, 5010 Duke Street, Alexandria, VA 22314

1 National Technical Information Service, 5285 Port Royal Road, Springfield, VA 22161

Battelle Columbus Laboratories, Metals and Ceramics Information Center, 505 King Avenue, Columbus, OH 45201
1 ATTN: Mr. Winston Duckworth
1 Dr. D. Niesz
1 Mr. H. Midim (MCIC)

Commander, Army Research Office, P.O. Box 12211, Research Triangle Park, NC 27709
2 ATTN: Information Processing Office
Dr. G. Meyer
Dr. F. Rothwarf

Commander, U.S. Army Tank-Automotive Command, Warren MI 48090
1 ATTN: Dr. W. Bryzik
1 Dr. H. Dobbs, Director

Commander, U.S. Army Mobility Equipment Research and Development Command, Fort Belvoir, VA 22060
1 ATTN: DRDME-EM, Mr. P. Arnold

Commander, U.S. Army Foreign Science and Technology Center, 220 7th Street, N.R., Charlottesville, VA 22901
1 ATTN: Military Tech, Mr. W. Marley

Chief of Naval Research, Arlington VA 22217
1 ATTN: Dr. A. Diness
1 Dr. R. Pohanka

Naval Research Laboratory, Washington, DC 20375
1 ATTN: Mr. D. Lewis

Commander, U.S. Air Force Wright Aeronautics Laboratory, Wright-Patterson Air Force Base, OH 45433, Dr. M. Lindey
1 ATTN: AFWAL/MLLM, Dr. H. Graham
AFWAL/MLLM, Dr. A. Katz
AFWAL/MLLM, Mr. K. Mazdiyasni

Copies

National Aeronautics and Space Administration, Lewis Research Center, 21000 Brookpark Road, Cleveland, OH 44135
1 ATTN: J. Accurio, USAMRDL

Department of Energy, Division of Transportation, 20 Massachusetts Avenue, N.W., Washington, DC 20545
3 ATTN: Mr. R. Schulz (TEC)
Mr. A. Chessness
Mr. C. Craig

National Research Council, National Materials Advisory Board, 2101 Constitution Avenue, Washington, DC 20418
1 ATTN: R. Spriggs
1 D. Groves

AiResearch Manufacturing Company, AiResearch Casting Company, 2525 West 190th Street, Torrance, CA 90505
1 ATTN: Mr. K. Styhr

Garrett Turbine Engine Company, Materials Engineering Dept., 111 South 34th Street, P.O. Box 5217, Phoenix, AZ 85010
1 ATTN: Dr. J. Wimmer, MS 93-393/503-4AL

SOHIO Engineered Materials (Carborundum)
P.O. Box 1054, Niagara Falls, NY 14302
1 ATTN: Mr. J. MacBeth
1 Mr. J. Hinton

Cummins Engine Company, Columbus, IN 47201
2 ATTN: Mr. T. Yonushonis
Dr. J. Patten

Synterials, Inc., 1821 Michael Faraday Drive, Reston, VA 22090
1 ATTN: Mr. R. Engdahl

Ford Motor Company, Turbine Research Department, 20000 Rotunda Drive, Dearborn, MI 48121
1 ATTN: Mr. A. McLean
1 Mr. T. Whelan
1 Mr. J. Mangels

Copies

General Electric Company, Research and Development Center, Box 8, Schenectady, NY 12345
1 ATTN: Dr. R. Charles
Dr. C. Greskovich

Georgia Institute of Technology, EES, Atlanta, GA 30332
1 ATTN: Mr. J. Walton

GTE Laboratories, Waltham Research Center, 40 Sylvan Road, Waltham, MA 02154
1 ATTN: Dr. J. Neal
1 Dr. J. Smith

IIT Research Institute, 10 West 35th Street, Chicago, IL 60616
1 ATTN: Mr. S. Bortz, Director, Ceramics Research

Caterpillar Tractor Co., Solar Division, 2200 Pacific Highway, P.O. Box 80966, San Diego, CA 92138
1 ATTN: Dr. A. Metcalfe

Kawecki Berylco Industries, Inc., P.O. Box 1462, Reading, PA 19603
1 ATTN: Mr. R. Longenecker

Massachusetts Institute of Technology, Department of Metallurgy and Materials Science, Cambridge, MA 02139
1 ATTN: Prof. R. Coble
1 Prof. H. Bowen
1 Prof. W. Kingery

Norton Company, Worcester, MA 01606
1 ATTN: Dr. J. Penzering
1 Dr. M. Torti

Pennsylvania State University, Material Science Department, University Park, PA 16802
1 ATTN: Prof. R. Tressler

Rockwell International Corporation, Science Center, 1049 Camino Dox Rios, Thousand Oaks, CA 91360
1 ATTN: Dr. F. Lange

United Technologies Research Center, East Harford, CT 06108
1 ATTN: Dr. J. Brennan

Copies

University of Washington, Ceramic Engineering Division, FB-10, Seattle, WA 98195
1 ATTN: Prof. J. Mueller
1 Prof. A. Miller

Westinghouse Electric Corporation, Research Laboratories, Pittsburgh, PA 15235
1 ATTN: Dr. R. Bratton

NASA Lewis Research Center, 21000 Brookpark Road, Cleveland, OH 44135
1 ATTN: T. Miller

Conservation and Advanced System Programs Metals and Ceramics Division, Oak Ridge National Laboratory, Nuclear Division, P.O. Box X, Oak Ridge, TN 37830
1 ATTN: Dr. T. Schaffhauser
1 Dr. V. Tennery
1 Dr. R. Johnson

General Motors Corporation, Detroit Diesel Allison, P.O. Box 894, Indianapolis, IN 46206
1 ATTN: P. Heitman, T-15
1 H. Helms (2 cps), T-15
1 R. Johnson, T-15

General Electric Company, Aircraft Engine Group, 1000 Western Avenue, Lynn, MA 01910
1 ATTN: A. Bellin (A-37428)

Pure Carbon Incorporated, St. Marys, PA 15856
1 ATTN: W. Shobert

U.S. Army Advance Concepts & Technology Office, HQDA (DAMA-ARZ-E), Washington, D.C. 20310
1 ATTN: Dr. C. Church

1 University of Washington, College of Engineering, Roberts Hall FB-10, Seattle, WA 98195
ATTN: Prof. R. Bradt

Copies

U.S. Army Materials Technology Laboratory, Watertown, MA 02172-0001

Copies		
2	ATTN:	SLCMT-IML
1		SLCMT-IMA-P
1		SLCMT-ISC
1		SLCMT-D, Dr. Wright
1		SLCMT-MCP, Dr. G. Quinn
1		SLCMT-MCS, Dr. G. Gazza
1		SLCMT-MC, Dr. Chait
10		SCLMT-MMC, Dr. Katz

U.S. Army Applied Technology Laboratory, Ft. Eustis, VA 23604-5577

1	ATTN:	Mr. H. Morrow
1		Mr. J. Lane

END

DTIC

8-86